arXiv:1511.07902v3 [stat.ML] 30 Jul 2016

Performance Limits of Online Stochastic Sub-Gradient Learning

Bicheng Ying YBC@UCLA.EDU
Ali H. Sayed SAYED@UCLA.EDU
Department of Electrical Engineering
University of California
Los Angeles, CA 90095, USA

Abstract

This work examines the performance of stochastic sub-gradient learning strategies under weaker conditions than usually considered in the literature. The conditions are shown to be automatically satisfied by several important cases of interest including the construction of Linear-SVM, LASSO, and Total-Variation denoising formulations. In comparison, these problems do not satisfy the traditional assumptions automatically and, therefore, conclusions derived based on these earlier assumptions are not directly applicable to these problems. The analysis establishes that stochastic sub-gradient strategies can attain exponential convergence rates, as opposed to sub-linear rates, to the steady-state. A realizable exponential-weighting procedure is proposed to smooth the intermediate iterates by the sub-gradient procedure and to guarantee the established performance bounds in terms of convergence rate and excessive risk performance. Both single-agent and multi-agent scenarios are studied, where the latter case assumes that a collection of agents are interconnected by a topology and can only interact locally with their neighbors. The theoretical conclusions are illustrated by several examples and simulations, including comparisons with the FISTA procedure.

Keywords: Sub-gradient, affine-Lipschitz, exponential rate, diffusion strategy, SVM, LASSO, Total Variation, FISTA

1. Introduction

The minimization of *non-differentiable* convex cost functions is a critical step in the solution of many design problems (Bertsekas, 1999; Polyak, 1987; Nesterov, 2004), including the design of sparse-aware (LASSO) solutions (Hastie et al., 2009; Tibshirani, 1996), support-vector machine (SVM) learners (Cortes and Vapnik, 1995; Shalev-Shwartz et al., 2011; Vapnik, 1998; Bishop, 2006; Theodoridis and Koutroumbas, 2008), or total-variation based image denoising solutions (Rudin et al., 1992; Beck and Teboulle, 2009a). Several powerful techniques have been proposed in the literature to deal with the non-differentiability aspect of the problem formulation, including methods that employ of sub-gradient iterations (Bertsekas, 1999; Polyak, 1987; Nesterov, 2004), cutting-plane techniques (Kelley, 1960), or proximal iterations (Parikh and Boyd, 2013; Bach et al., 2012). This work focuses on the class of sub-gradient methods for the reasons explained in the sequel. The sub-gradient technique is closely related to the traditional gradient-descent method where the actual gradient is replaced by a sub-gradient at the points of non-differentiability. It is one of the

simplest methods in current practice but is known to suffer from slow convergence. For instance, it is shown in (Nesterov, 2004) that, for convex cost functions, the optimal convergence rate that can be delivered by sub-gradient methods in *deterministic* optimization problems cannot be faster than $O(1/\sqrt{i})$, where i is the iteration index.

Still, there are at least three strong reasons that motivate a closer examination of the limits of performance of sub-gradient learning algorithms. First, the explosive interest in large-scale and big data scenarios favors the use of simple and computer-efficient algorithmic structures, of which the sub-gradient technique is a formidable example. Second, it is becoming increasingly evident that more sophisticated optimization iterations do not necessarily ensure improved performance when dealing with complex models and data structures (Bousquet and Bottou, 2008; Bottou, 2012; Polyak, 1987; Towfic and Sayed, 2015). This is because the assumed models, or the adopted cost functions, do not always reflect faithfully the underlying problem structure. In addition, the presence of noise in the data generally implies that a solution that may be perceived to be optimal is actually sub-optimal due to perturbations in the data and models. Third, it turns out that a clear distinction needs to be made between optimizing *deterministic* costs (Bertsekas, 1999; Polyak, 1987; Nesterov, 2004), where the cost function is known completely beforehand, and optimizing *stochastic* costs, where the cost function is actually unavailable due to its dependence on the unknown probability distribution of the data. Stochastic problem formulations are very common in applications arising in machine learning problems, adaptation, and estimation. We will show that sub-gradient algorithms have surprisingly favorable behavior in the stochastic setting.

Motivated by these remarks, we therefore examine in some detail the performance of *stochastic sub-gradient* algorithms for the minimization of non-differentiable convex costs. Our analysis will reveal some interesting properties when these algorithms are used in the context of continuous adaptation and learning (i.e., when actual sub-gradients cannot be evaluated but need to be *approximated* continually in an *online* manner). The study is carried out for both cases of single stand-alone agents and multi-agent networks (Sayed, 2014a; Chen and Sayed, 2015a,b; Nedic and Ozdaglar, 2009; Ram et al., 2010). We start with single-agent learning and establish some revealing conclusions about how fast and how well the agent is able to learn. Extension of the results to the multi-agent case will require additional effort due to the coupling that exists among neighboring agents. Nevertheless, the same broad conclusions will continue to hold in this case with proper adjustments.

In order to examine the performance of *stochastic* sub-gradient implementations, it is necessary to introduce some assumptions on the gradient noise process (which is the difference between a true sub-gradient and its approximation). Here we diverge in a noticeable way from assumptions commonly used in the literature for two reasons (see Sec. 3 for further explanations). First, we introduce weaker assumptions than usually adopted in prior works and, secondly and more importantly, we show that our assumptions are automatically satisfied for important cases of interest (such as SVM, LASSO, Total Variation). In contrast, these applications do not satisfy the traditional assumptions used in the literature and, therefore, conclusions derived based on these earlier assumptions are not directly applicable to these problems. For example, it is common in the literature to assume that the cost function has a bounded gradient (Nemirovski et al., 2009; Boyd and Mutapcic, 2008; Polyak, 1987; Ram et al., 2010; Nedic and Ozdaglar, 2009; Agarwal et al., 2012); this condition is

not even satisfied by quadratic costs whose gradient vectors are affine in their parameter. This condition is also in direct conflict with strongly-convex costs (Agarwal et al., 2012). By weakening the assumptions, the analysis in this work becomes more challenging (as the material in the appendices reveal). At the same time, the conclusions become stronger and more revealing, and they apply to a broader class of algorithms and scenarios.

A second aspect of our study is that we focus on the use of *constant* step-sizes in order to enable continuous adaptation and learning. Since the step-size is assumed to remain constant, the effect of gradient noise is always present and does not die out, as would occur if we were using instead a diminishing step-size, say, of the form $\mu(i) = \tau/i$ for some $\tau > 0$ (Shalev-Shwartz et al., 2011; Boyd and Mutapcic, 2008; Nedic and Ozdaglar, 2009). Such diminishing step-sizes annihilate the gradient noise term asymptotically albeit at the cost of turning off adaptation in the long run. When this happens, the learning algorithm loses its ability to track drifts in the solution. In contrast, a constant step-size keeps adaptation alive and endows the learning algorithm with an inherent tracking mechanism: if the minimizer that we are seeking drifts with time due, for example, to changes in the statistical properties of the data, then the algorithm will be able to track the new location since it is continually adapting (Sayed, 2008). This useful tracking feature comes at the expense of a persistent gradient noise term that never dies out. The challenge in analyzing the performance of learning algorithms in the constant adaptation regime is to show that their feedback mechanism induces a stable behavior that reduces the size (variance) of the gradient noise to a small level and that ensures convergence of the iterates to within $O(\mu)$ of the desired optimal solution. Moreover, and importantly, it turns out that constant step-size adaptation is not only useful under non-stationary conditions when drifts in the data occur, but it is also useful even under stationary conditions when the minimizer does not vary with time. This is because, as we will see, the convergence towards the steady-state regime will now be guaranteed to occur at an exponential rate, $O(\alpha^i)$ for some $\alpha \in (0, 1)$, which is much faster than the $O(1/i)$ rate that would be observed under a diminishing step-size implementation for strongly-convex costs.

A third aspect of our contribution is that it is known that sub-gradient methods are not *descent* methods. For this reason, it is customary to employ pocket variables (i.e., the best iterate)(Bertsekas, 1999; Nesterov, 2004; Shor, 2012; Kiwiel, 1985) or arithmetic averages (Shalev-Shwartz et al., 2011) to smooth out the output. However, as the analysis will reveal, the pocket method is not practical in the *stochastic* setting (its implementation requires knowledge of unavailable information), and the use of arithmetic averages (Moulines and Bach, 2011) does not match the convergence rate derived later in Sec. 4.3. We shall propose an alternative weighted averaging scheme with an exponentially-decaying weight and show that this technique does not degrade convergence while providing the desired smoothing effect.

Notation: We use lowercase letters to denote vectors, uppercase letters for matrices, plain letters for deterministic variables, and boldface letters for random variables. We also use $(\cdot)^{\mathsf{T}}$ to denote transposition, $(\cdot)^{-1}$ for matrix inversion, $\mathsf{Tr}(\cdot)$ for the trace of a matrix, $\lambda(\cdot)$ for the eigenvalues of a matrix, $\|\cdot\|$ for the 2-norm of a matrix or the Euclidean norm of a vector, and $\rho(\cdot)$ for the spectral radius of a matrix. Besides, we use $A \geq B$ to denote that $A - B$ is positive semi-definite, and $p \succ 0$ to denote that all entries of vector p are positive.

2. Problem Formulation: Single Agent Case

2.1 Problem Formulation

We consider the problem of minimizing a risk function, $J(w) : \mathbb{R}^M \to \mathbb{R}$, which is assumed to be expressed as the expected value of some loss function, $Q(w; \boldsymbol{x})$, namely,

$$w^\star \triangleq \arg\min_w J(w), \tag{1}$$

where we assume $J(w)$ is strongly convex with its unique minimizer denoted by $w^\star$, and where

$$J(w) \triangleq \mathbb{E}\, Q(w; \boldsymbol{x}). \tag{2}$$

Here, the letter $\boldsymbol{x}$ represents the random data and the expectation operation is performed over the distribution of this data. Many problems in adaptation and learning involve risk functions of this form, including, for example, mean-square-error designs and support vector machine (SVM) solutions — see, e.g., (Sayed, 2008; Theodoridis and Koutroumbas, 2008; Bishop, 2006). For generality, we allow the risk function $J(w)$ to be *non-differentiable*. This situation is common in machine learning formulations, e.g., in SVM costs and in regularized sparsity-inducing formulations; examples to this effect are provided in the sequel.

In this work, we examine in some detail the performance of stochastic *sub-gradient* algorithms for the minimization of (1) and reveal some interesting properties when these algorithms are used in the context of continuous adaptation and learning (i.e., when actual sub-gradients cannot be evaluated but need to be *approximated* continually in an online manner). This situation arises when the probability distribution of the data is not known beforehand, as is common in practice. In most applications, we only have access to data realizations but not to their actual distribution. Our study is carried out for both cases of single stand-alone agents and multi-agent networks. We start with single-agent learning and establish some revealing conclusions about how fast and how well the agent is able to learn. Extension of the results to the multi-agent case will require additional effort due to the coupling that exists among neighboring agents, and is pursued in a future section. The same broad conclusions will continue to hold in this case as well with some proper adjustments.

2.2 Stochastic Sub-Gradient Algorithm

To describe the sub-gradient algorithm in the single-agent case, we first recall that the sub-gradient of a convex function $J(w)$ at any arbitrary point w_0 is defined as any vector $g \in \mathbb{R}^M$ that satisfies:

$$J(w) \;\geq\; J(w_0) + g^{\mathsf{T}}(w - w_0), \;\; \forall w \tag{3}$$

We shall often write $g(w_0)$, instead of simply g, in order to emphasize that it is a sub-gradient vector at location w_0. We note that sub-gradients are generally non-unique. Accordingly, a related concept is that of the *sub-differential* of $J(w)$ at w_0, denoted by $\partial J(w_0)$. The sub-differential is defined as the set of all possible sub-gradient vectors at w_0:

$$\partial J(w_0) \triangleq \Big\{ g \mid J(w) \geq J(w_0) + g^{\mathsf{T}}(w - w_0), \;\; \forall w \Big\}. \tag{4}$$

In general, the sub-differential $\partial J(w_0)$ is a set and it will collapse to a single point if, and only if, the cost function is differentiable at w_0(Nesterov, 2004); in that case, the sub-gradient vector will coincide with the actual gradient vector at location w_0.

Referring back to problem (1), the traditional sub-gradient method to minimizing the risk function $J(w)$ takes the form:

$$w_i = w_{i-1} - \mu\, g(w_{i-1}), \quad i \geq 0 \tag{5}$$

where $g(w_{i-1})$ refers to one particular choice of a sub-gradient vector for $J(w)$ at location w_{i-1}, and $\mu > 0$ is a small step-size parameter. Since sub-gradients are non-unique, in construction (5), it is assumed that once a form for $g(w)$ is selected, that choice remains invariant throughout the adaptation process. That is, the user selects one choice for $g(w)$ and sticks to it throughout the adaptation process. It is not the case that $g(w)$ can sometimes be chosen in one way in one iteration and then in another way in another iteration. Now, in the context of adaptation and learning, we usually do not know the exact form of $J(w)$ because the distribution of the data is not known to enable computation of $\mathbb{E}\, Q(w; \boldsymbol{x})$. As such, true sub-gradient vectors for $J(w)$ cannot be determined and they will need to be replaced by stochastic approximations evaluated from streaming data; examples to this effect are provided in the sequel in the context of support-vector machines and LASSO sparse designs. Accordingly, we replace the deterministic iteration (5) by the following stochastic iteration(Bertsekas, 1999; Nesterov, 2004; Shor, 2012; Kiwiel, 1985):

$$\boldsymbol{w}_i = \boldsymbol{w}_{i-1} - \mu\, \widehat{g}(\boldsymbol{w}_{i-1}), \tag{6}$$

where the successive iterates, $\{\boldsymbol{w}_i\}$, are now random variables (denoted in boldface) and $\widehat{g}(\cdot)$ represents an approximate sub-gradient vector at location $\boldsymbol{w}_{i-1}$ estimated from data available at time i. The difference between an actual sub-gradient vector and its approximation is referred to as *gradient noise* and is denoted by

$$\boldsymbol{s}_i(\boldsymbol{w}_{i-1}) \;\stackrel{\Delta}{=}\; \widehat{g}(\boldsymbol{w}_{i-1}) - g(\boldsymbol{w}_{i-1}). \tag{7}$$

where the notation $\widehat{g}(\boldsymbol{w}_{i-1})$ refers to the approximation adopted for the particular sub-gradient vector used in (5). We will clarify this construction below in Section 2.3 and provide illustrative examples.

2.3 Examples: SVM and LASSO

To illustrate the construction, we list two examples dealing with support vector machines (SVM) (Cortes and Vapnik, 1995) and the LASSO problem (Tibshirani, 1996); the latter is also known as the sparse LMS problem or basis pursuit (Chen et al., 2009, 1998; Hastie et al., 2009). We will be using these two problems throughout the manuscript to illustrate our findings.

Example 1 (SVM problem). The two-class SVM formulation deals with the problem of determining a separating hyperplane, $w \in \mathbb{R}^M$, in order to classify feature vectors, denoted by $\boldsymbol{h} \in \mathbb{R}^M$, into one of two classes: $\boldsymbol{\gamma} = +1$ or $\boldsymbol{\gamma} = -1$. The regularized SVM risk function is of the form:

$$J^{\rm svm}(w) \quad \stackrel{\Delta}{=} \quad \frac{\rho}{2}\|w\|^2 + \mathbb{E}\left(\max\left\{0, 1 - \boldsymbol{\gamma}\boldsymbol{h}^{\mathsf{T}} w\right\}\right), \tag{8}$$

where $\rho > 0$ is a regularization parameter. We are generally given a collection of independent training data, $\{\boldsymbol{\gamma}(i), \boldsymbol{h}_i\}$, consisting of feature vectors and their class designations and assumed to arise from joint wide-sense stationary processes. Using this data, the loss function at time i is given by

$$Q^{\rm svm}(w; \{\boldsymbol{\gamma}(i), \boldsymbol{h}_i\}) = \frac{\rho}{2}\|w\|^2 + \max\left\{0, 1 - \boldsymbol{\gamma}(i)\boldsymbol{h}_i^{\mathsf{T}} w\right\}, \tag{9}$$

where the second term on the right-hand side, which is also known as the hinge function, is non-differentiable at all points w satisfying $1 - \boldsymbol{\gamma}(i)\boldsymbol{h}_i^{\mathsf{T}} w = 0$. There are generally many choices for the sub-gradient vector at these locations w. One particular choice is

$$g^{\rm svm}(\boldsymbol{w}_{i-1}) = \rho \boldsymbol{w}_{i-1} + \mathbb{E}\,\boldsymbol{\gamma}\boldsymbol{h}\,\mathbb{I}[\boldsymbol{\gamma}\boldsymbol{h}^{\mathsf{T}}\boldsymbol{w}_{i-1} \leq 1], \tag{10}$$

where the indicator function $\mathbb{I}[a]$ is defined as follows:

$$\mathbb{I}[a] \;=\; \left\{ \begin{array}{ll} 1, & \text{if statement } a \text{ is true} \\ 0, & \text{otherwise} \end{array} \right. \tag{11}$$

The choice (10) requires the computation of an expectation operator, which is infeasible since the distribution of the data is not known beforehand. One approximation for this particular sub-gradient choice is the construction

$$\widehat{g}^{\rm svm}(\boldsymbol{w}_{i-1}) = \rho \boldsymbol{w}_{i-1} + \boldsymbol{\gamma}(i)\boldsymbol{h}_i\,\mathbb{I}[\boldsymbol{\gamma}(i)\boldsymbol{h}_i^{\mathsf{T}}\boldsymbol{w}_{i-1} \leq 1], \tag{12}$$

where the expectation operator is dropped. We refer to (12) as an instantaneous approximation for (10) since it employs the instantaneous realizations $\{\boldsymbol{\gamma}(i), \boldsymbol{h}_i\}$ to approximate the mean operation in (10). There can be other choices for the true sub-gradient vector at $\boldsymbol{w}_{i-1}$ and for its approximation. However, it is assumed that once a particular choice is made for the form of $g(\boldsymbol{w}_{i-1})$, as in (10), then that form and its approximation (12) remain invariant during the operation of the algorithm. Using (10) and (12), the gradient noise process associated with this implementation of the SVM formulation is then given by

$$\boldsymbol{s}_i^{\rm svm}(\boldsymbol{w}_{i-1}) = \boldsymbol{\gamma}(i)\boldsymbol{h}_i\,\mathbb{I}[\boldsymbol{\gamma}(i)\boldsymbol{h}_i^{\mathsf{T}}\boldsymbol{w}_{i-1} \leq 1] - \mathbb{E}\,\boldsymbol{\gamma}\boldsymbol{h}\,\mathbb{I}[\boldsymbol{\gamma}\boldsymbol{h}^{\mathsf{T}}\boldsymbol{w}_{i-1} \leq 1]. \tag{13}$$

□

Example 2 (LASSO problem). The least-mean-squares LASSO formulation deals with the problem of estimating a sparse weight vector by minimizing a risk function of the form (Donoho et al., 2006; Murakami et al., 2010):[1]

$$J^{\rm lasso}(w) \;\triangleq\; \frac{1}{2}\mathbb{E}\,\|\boldsymbol{\gamma} - \boldsymbol{h}^{\mathsf{T}} w\|^2 + \delta\|w\|_1, \tag{14}$$

where $\delta > 0$ is a regularization parameter and $\|w\|_1$ denotes the ℓ_1-norm of w. In this problem formulation, the variable $\boldsymbol{\gamma}$ now plays the role of a desired signal, while $\boldsymbol{h}$ plays the role of a regression vector. It is assumed that the data are zero-mean wide-sense stationary with second-order moments denoted by

$$\boldsymbol{r}_{h\gamma} \;\triangleq\; \mathbb{E}\,\boldsymbol{h}\boldsymbol{\gamma}, \quad R_h \;\triangleq\; \mathbb{E}\,\boldsymbol{h}\boldsymbol{h}^{\mathsf{T}}. \tag{15}$$

1. Traditionally, LASSO refers to minimize a deterministic cost function, like $\|y - Ax\|^2 + \lambda\|x\|_1$. However, since here we are more interested in stochastic version, we only consider the case like (14).

It is generally assumed that $\{\boldsymbol{\gamma}, \boldsymbol{h}\}$ satisfy a linear regression model of the form:

$$\boldsymbol{\gamma} = \boldsymbol{h}^{\mathsf{T}} w^o + \boldsymbol{n}, \tag{16}$$

where $w^o \in \mathbb{R}^M$ is the desired unknown sparse vector, and $\boldsymbol{n}$ refers to an additive zero-mean noise component with finite variance σ_n^2 and independent of $\boldsymbol{h}$. If we multiply both sides of (16) by $\boldsymbol{h}$ from the left and compute expectations, we find that w^o satisfies the normal equations:

$$r_{h\gamma} = R_h w^o. \tag{17}$$

We are again given a collection of independent training data, $\{\boldsymbol{\gamma}(i), \boldsymbol{h}_i\}$, consisting of regression vectors and their noisy measured signals. Using this data, the loss function at time i is given by

$$Q^{\text{lasso}}(w; \{\boldsymbol{\gamma}(i), \boldsymbol{h}_i\}) = \frac{1}{2}(\boldsymbol{\gamma}(i) - \boldsymbol{h}_i^{\mathsf{T}} w)^2 + \delta \|w\|_1, \tag{18}$$

where the second term on the right-hand side is again non-differentiable. One particular choice for the sub-gradient vector is:

$$\begin{aligned} g^{\text{lasso}}(\boldsymbol{w}_{i-1}) &= -\mathbb{E}\, \boldsymbol{h}(\boldsymbol{\gamma} - \boldsymbol{h}^{\mathsf{T}} \boldsymbol{w}_{i-1}) + \delta \cdot \text{sgn}(\boldsymbol{w}_{i-1}) \\ &= -R_h(w^o - \boldsymbol{w}_{i-1}) + \delta \cdot \text{sgn}(\boldsymbol{w}_{i-1}) \end{aligned} \tag{19}$$

where the notation $\text{sgn}(a)$, for a scalar a, refers to the sign function:

$$\text{sgn}[a] = \begin{cases} +1, & a \geq 0 \\ -1, & \text{otherwise.} \end{cases} \tag{20}$$

When applied to a vector a, as is the case in (19), the sgn function is a vector consisting of the signs of the individual entries of a. Similar to the previous example, it is infeasible to find the exact sub-graident (19) since R_h is unknown. Instead, we use the following instantaneous approximation for (19):

$$\begin{aligned} \widehat{g}^{\text{lasso}}(\boldsymbol{w}_{i-1}) &= -\boldsymbol{h}_i(\boldsymbol{\gamma}(i) - \boldsymbol{h}_i^{\mathsf{T}} \boldsymbol{w}_{i-1}) + \delta \cdot \text{sgn}(\boldsymbol{w}_{i-1}) \\ &= -\boldsymbol{h}_i \boldsymbol{h}_i^{\mathsf{T}}(w^\circ - \boldsymbol{w}_{i-1}) + \delta \cdot \text{sgn}(\boldsymbol{w}_{i-1}) - \boldsymbol{h}_i \boldsymbol{n}(i). \end{aligned} \tag{21}$$

It then follows that the gradient noise process in the LASSO formulation is given by

$$\boldsymbol{s}_i^{\text{lasso}}(\boldsymbol{w}_{i-1}) = (R_h - \boldsymbol{h}_i \boldsymbol{h}_i^{\mathsf{T}})(w^\circ - \boldsymbol{w}_{i-1}) - \boldsymbol{h}_i \boldsymbol{n}(i). \tag{22}$$

□

3. Modeling Conditions

In order to examine the performance of the stochastic sub-gradient implementation (6) for single-agent adaptation and learning, and later for multi-agent networks, it is necessary to introduce some assumptions on the gradient noise process. We diverge here from assumptions that are commonly used in the literature for two reasons. First, we introduce weaker assumptions than usually adopted in prior works and, secondly and more importantly, we show that our assumptions are automatically satisfied by important cases of interest (such as

SVM and LASSO). In contrast, these applications do not satisfy the traditional assumptions used in the literature and, therefore, conclusions derived based on these earlier assumptions are not directly applicable to SVM and LASSO problems. We clarify these remarks in the sequel.

First, we emphasize, as explained above, that it is assumed that the particular choice for the sub-gradient function at location $\boldsymbol{w}_{i-1}$ remains invariant during the operation of the algorithm, as well as its instantaneous approximation. Now, recall from (1) that $w^\star$ denotes the global minimizer that we are seeking. The first set of conditions on the gradient noise process below essentially require that the construction of the approximate sub-gradient vector should not introduce bias and that its error variance should decrease as the quality of the iterate approaches the optimal solution, $w^\star$. Both of these conditions are sensible and, moreover, they will be shown to be satisfied by, for example, SVM and LASSO constructions. More formally, we require the gradient noise process to satisfy the following two conditions.

Assumption 1 (Conditions on gradient noise) *The first and second-order conditional moments of the gradient noise process satisfy the following conditions:*

$$\begin{aligned} \mathbb{E}\,[\,s_i(\boldsymbol{w}_{i-1})\,|\,\boldsymbol{\mathcal{F}}_{i-1}\,] &= 0, &(23)\\ \mathbb{E}\,[\,\|s_i(\boldsymbol{w}_{i-1})\|^2\,|\,\boldsymbol{\mathcal{F}}_{i-1}\,] &\leq \beta^2\|w^\star-\boldsymbol{w}_{i-1}\|^2+\sigma^2, &(24)\end{aligned}$$

for some constants $\beta^2 \geq 0$ and $\sigma^2 \geq 0$, and where the notation $\boldsymbol{\mathcal{F}}_{i-1}$ denotes the filtration (collection) corresponding to all past iterates:

$$\boldsymbol{\mathcal{F}}_{i-1} \;=\; \text{filtration by } \{\boldsymbol{w}_j,\; j \leq i-1\}. \tag{25}$$

■

Assumption 2 (Strongly-convex risk function) *The risk function is assumed to be $\eta-$strongly-convex (or, simply, strongly-convex), i.e., there exists an $\eta > 0$ such that*

$$J(\theta w_1+(1-\theta)w_2) \;\leq\; \theta J(w_1)+(1-\theta)J(w_2)-\frac{\eta}{2}\theta(1-\theta)\|w_1-w_2\|^2, \tag{26}$$

for any $\theta \in [0,1]$, w_1, and w_2. The above condition is equivalent to requiring (Polyak, 1987):

$$J(w_1) \geq J(w_2)+g(w_2)^{\mathsf{T}}(w_1-w_2)+\frac{\eta}{2}\|w_1-w_2\|^2. \tag{27}$$

Under this condition, the minimizer $w^\star$ exists and is unique. ■

Assumption 2 is relatively rare in works on non-differentiable function optimization because it is customary for these works to focus on studying *piece-wise* linear risks; these are important examples of non-smooth functions but they do not satisfy the strong-convexity condition. In our case, strong-convexity is not a restriction because in the context of adaptation and learning, it is common for the risk functions to include a regularization term, which generally helps ensure strong-convexity.

Assumption 3 (Sub-gradient is Strictly Affine-Lipschitz) *It is assumed that the sub-gradient choice used in (5) is affine Lipschitz, meaning that there exist constants $c \geq 0$ and $d \geq 0$ such that*

$$\|g(w_1) - g'(w_2)\| \;\leq\; c\|w_1 - w_2\| + d, \quad \forall w_1, w_2, \tag{28}$$

holds for any $g'(\cdot) \in \partial J(\cdot)$. ■

More critically, though, it is customary in the literature to use in place of Assumption 3 a more restrictive condition that requires the sub-gradient to be bounded (Bertsekas, 1999; Nedic and Ozdaglar, 2009; Nemirovski et al., 2009; Ram et al., 2010; Agarwal et al., 2012), i.e.,

$$\|g(w)\| \leq d_1, \quad \forall w,\; g(w) \in \partial J(w). \tag{29}$$

which is also equivalent to assuming the risk function is Lipschitz:

$$\|J(w_1) - J(w_2)\| \leq d_1\|w_1 - w_2\|, \quad \forall w_1, w_2 \tag{30}$$

Such a requirement does not even hold for quadratic risk functions, $J(w)$, whose gradient vectors are affine in w and, therefore, grow unbounded! Even more, it can be easily seen that requirement (29) is always conflicted with the strong-convexity assumption. For example, if we set $w_1 = w$ and $w_2 = w^\star$ in (27), we would obtain:

$$J(w) \geq J(w^\star) + \frac{\eta}{2}\|w - w^\star\|^2. \tag{31}$$

Likewise, if we instead set $w_1 = w^\star$ and $w_2 = w$ in (27), we would obtain:

$$J(w^\star) \geq J(w) + g(w)^{\mathsf{T}}(w^\star - w) + \frac{\eta}{2}\|w - w^\star\|^2. \tag{32}$$

Adding relations (31)–(32) we arrive at the so-called strong monotonicity property:

$$g(w)^{\mathsf{T}}(w - w^\star) \quad \geq \quad \eta\|w - w^\star\|^2, \tag{33}$$

which implies, in view of the Cauchy-Schwarz inequality, that

$$\|g(w)\| \geq \eta\|w - w^\star\|. \tag{34}$$

In other words, the strong-convexity condition (27) implies that the sub-gradient satisfies (34); and this condition is in clear conflict with the bounded requirement in (29).

One way to circumvent this problem is to restrict the domain of $J(w)$ to some bounded convex set, say, $w \in \mathcal{W}$, in order to bound its sub-gradient vectors, and then employ a projection-based sub-gradient method (i.e., one in which each iteration is followed by projecting $\boldsymbol{w}_i$ onto $\mathcal{W}$). However, this approach has at least three difficulties. First, the unconstrained problem is transformed into a more demanding constrained problem involving an extra projection step. Second, the projection step may not be straightforward to carry out unless the set $\mathcal{W}$ is simple enough. Third, the bound that results on the sub-gradient vectors by limiting w to $\mathcal{W}$ can be very loose, which will be dependent on the diameter of convex set $\mathcal{W}$.

For these reasons, we do not rely on the restrictive condition (29) and introduce instead the more relaxed affine-Lipschitz condition (28). This condition is weaker than (29). Indeed, it can be verified that (29) implies (28) but not the other way around. To see this, assume (29) holds. Then, using the triangle inequality of norms we have

$$\begin{aligned}\|g(w_1) - g'(w_2)\| &\leq \|g(w_1)\| + \|g'(w_2)\| \\ &\leq d_1 \ + \ d_1 \\ &= 2d_1, \end{aligned} \tag{35}$$

which is a special case of (28) with $c = 0$ and $d = 2d_1$. We now verify that important problems of interest satisfy Assumption 3 but *not* the traditional condition (29).

Example 3 (SVM problem). We revisit the SVM formulation from Example 1. The risk function (8) is strongly convex due to the presence of the quadratic regularization term, $\frac{\rho}{2}\|w\|^2$, and since the hinge function $\mathbb{E}\max\{0, 1-\boldsymbol{\gamma}\boldsymbol{h}^{\mathsf{T}}w\}$ is convex. The zero-mean property of the gradient noise process is obvious in this case. With respect to the variance condition, we note that

$$\begin{aligned}\mathbb{E}\,[\|s_i^{\mathrm{svm}}(\boldsymbol{w}_{i-1})\|^2|\boldsymbol{\mathcal{F}}_{i-1}] &= \mathbb{E}\,\boldsymbol{h}_i^{\mathsf{T}}\boldsymbol{h}_i\,\mathbb{I}[\boldsymbol{\gamma}(i)\boldsymbol{h}_i^{\mathsf{T}}\boldsymbol{w}_{i-1} \leq 1] - \|\mathbb{E}\,\boldsymbol{\gamma}\boldsymbol{h}\,\mathbb{I}[\boldsymbol{\gamma}\boldsymbol{h}^{\mathsf{T}}\boldsymbol{w}_{i-1} \leq 1]\|^2 \\ &\leq \mathbb{E}\,\boldsymbol{h}_i^{\mathsf{T}}\boldsymbol{h}_i\,\mathbb{I}[\boldsymbol{\gamma}(i)\boldsymbol{h}_i^{\mathsf{T}}\boldsymbol{w}_{i-1} \leq 1] \\ &\leq \mathbb{E}\,\boldsymbol{h}_i^{\mathsf{T}}\boldsymbol{h}_i \\ &= \mathrm{Tr}(R_h), \end{aligned} \tag{36}$$

so that Assumption 1 is satisfied with $\beta^2 = 0$ and $\sigma^2 = \mathrm{Tr}(R_h)$. Let us now verify Assumption 3. For that purpose, we first note that the sub-differentiable set of the SVM risk can be described by:

$$\begin{aligned}\partial_w\,\mathbb{E}\,Q^{\mathrm{svm}}\big(w;\boldsymbol{h}=h,\boldsymbol{\gamma}=\gamma\big) &\overset{(a)}{=} \mathbb{E}\,\partial_w\,Q^{\mathrm{svm}}\big(w;\boldsymbol{h}=h,\boldsymbol{\gamma}=\gamma\big) \qquad (37)\\ &= \rho w + \mathbb{E}\,\partial_w\left(\max\left\{0, 1-\boldsymbol{\gamma}\boldsymbol{h}^{\mathsf{T}}w\right\}\right) \\ &\overset{(b)}{=} \rho w - \mathbb{E}\,\boldsymbol{\gamma}\boldsymbol{h}\cdot\mathcal{T}_1(1-\boldsymbol{\gamma}\boldsymbol{h}^{\mathsf{T}}w) \qquad (38)\end{aligned}$$

where in step (a), we use the fact that the SVM loss function is continuous convex and, therefore, we can exchange the order of the sub-differential operation with the expectation operation (Wets, 1989, Prop. 2.10); in step (b), the operator $\mathcal{T}_1$ is defined by

$$\mathcal{T}_1(x) \ \triangleq \ \begin{cases} 1, & x > 0 \\ [0,1], & x = 0 \\ 0, & x < 0 \end{cases} \tag{39}$$

Different choices for the value of $\mathcal{T}_1(x)$ at location $x = 0$ lead to different sub-gradients. We can therefore express any arbitrary sub-gradient in the form

$$g^{\mathrm{svm}\prime}(w) = \rho w - \mathbb{E}\,\boldsymbol{\gamma}\boldsymbol{h}\cdot\mathcal{T}_1'(1-\boldsymbol{\gamma}\boldsymbol{h}^{\mathsf{T}}w) \tag{40}$$

where the notation $\mathcal{T}_1'(x)$ means that we pick a particular value within the range $[0,1]$ to define the sub-gradient (40). It now follows that

$$\|g^{\rm svm}(w_1) - g^{\rm svm\prime}(w_2)\| \leq \rho\|w_1 - w_2\| + \big\|\mathbb{E}\,\boldsymbol{\gamma h}\,\mathbb{I}[\boldsymbol{\gamma h}^{\mathsf{T}}\boldsymbol{w}_{i-1} \leq 1]\big\| + \big\|\mathbb{E}\,\boldsymbol{\gamma h}\cdot\mathcal{T}_1'(1-\boldsymbol{\gamma h}^{\mathsf{T}}w)\big\|. \tag{41}$$

Now note that:

$$\begin{aligned}\big\|\mathbb{E}\,\boldsymbol{\gamma h}\cdot\mathcal{T}_1'(1-\boldsymbol{\gamma h}^{\mathsf{T}}w)\big\|^2 &\leq \mathbb{E}\,\|\boldsymbol{\gamma h}\cdot\mathcal{T}_1'(1-\boldsymbol{\gamma h}^{\mathsf{T}}w)\|^2\\ &= \mathbb{E}\,\boldsymbol{h}^{\mathsf{T}}\boldsymbol{h}\cdot[\mathcal{T}_1'(1-\boldsymbol{\gamma h}^{\mathsf{T}}w)]^2\\ &\leq \mathbb{E}\,\boldsymbol{h}^{\mathsf{T}}\boldsymbol{h}\\ &= {\rm Tr}(R_h)\end{aligned} \tag{42}$$

where the last inequality is because $\boldsymbol{h}^{\mathsf{T}}\boldsymbol{h}$ is non-negative and $[\mathcal{T}_1'(x)]^2$ is uniformly bounded by one. Substituting into (41) gives

$$\|g^{\rm svm}(w_1) - g^{\rm svm\prime}(w_2)\| \leq \rho\|w_1 - w_2\| + 2[{\rm Tr}(R_h)]^{1/2}, \tag{43}$$

which is of the same form as (28) with parameters $c=\rho$ and $d = 2[{\rm Tr}(R_h)]^{1/2}$. □

Example 4 (LASSO problem). We revisit the LASSO formulation from Example 2. Under the condition that $R_h > 0$, the risk function (14) is again strongly-convex because the quadratic term, $\frac{1}{2}\mathbb{E}\,\|\boldsymbol{\gamma} - \boldsymbol{h}^{\mathsf{T}}w\|^2$, is strongly convex and the regularization term, $\delta\|w\|_1$, is convex. With regards to the gradient noise process, it was already shown in Eq. (3.22) in (Sayed, 2014a) that a gradient noise process of the form (22) is zero-mean and its conditional variance satisfies:

$$\begin{aligned}\mathbb{E}\,[\|s_i^{\rm lasso}(\boldsymbol{w}_{i-1})\|^2|\boldsymbol{\mathcal{F}}_{i-1}] &\leq a\|w^\circ - \boldsymbol{w}_{i-1}\|^2 + \sigma_n^2{\rm Tr}(R_h)\\ &\leq 2a\|w^\star - \boldsymbol{w}_{i-1}\|^2 + \sigma_n^2{\rm Tr}(R_h) + 2a\|w^\circ - w^\star\|^2,\end{aligned} \tag{44}$$

where $a = 2\mathbb{E}\,\|R_h - \boldsymbol{h}_i\boldsymbol{h}_i^{\mathsf{T}}\|^2$. It follows that Assumption 1 is satisfied with $\beta^2 = 2a$ and $\sigma^2 = \sigma_n^2{\rm Tr}(R_h) + 2a\|w^\circ - w^\star\|^2$. Let us now verify Assumption 3. For that purpose, we first note that the sub-differential set of LASSO risk is given by:

$$\begin{aligned}\partial_w J^{\rm lasso}(w) &= -\mathbb{E}\,\boldsymbol{h}(\boldsymbol{\gamma} - \boldsymbol{h}^{\mathsf{T}}w) + \delta\cdot\mathcal{T}_2(w)\\ &= -R_h(w^o - w) + \delta\cdot\mathcal{T}_2(w)\end{aligned} \tag{45}$$

where the operator $\mathcal{T}_2(x)$ for a vector x is defined as:

$$\mathcal{T}_2(x) \;\triangleq\; \begin{bmatrix}\mathcal{T}_2(x(1))\\ \mathcal{T}_2(x(2))\\ \vdots\\ \mathcal{T}_2(x(M))\end{bmatrix}, \quad \mathcal{T}_2(x(i)) \;\triangleq\; \begin{cases}1, & x(i) > 0\\ [-1,1], & x(i) = 0\\ -1, & x(i) < 0\end{cases} \tag{46}$$

Different choices for the value of $\mathcal{T}_2(x)$ at the locations $x(i) = 0$ lead to different sub-gradients. We can therefore express any arbitrary sub-gradient in the form

$$g^{\rm lasso\prime}(w) = -R_h(w^o - w) + \delta\cdot\mathcal{T}_2'(w) \tag{47}$$

where the notation $\mathcal{T}_2'(x)$ means that we pick particular values within the range $[-1,1]$ to define the sub-gradient (47). It now follows that:

$$\|g^{\text{lasso}}(w_1) - g^{\text{lasso}'}(w_2)\| = \|R_h w_1 - R_h w_2 + \delta \cdot \big(\text{sgn}(w_1) - \mathcal{T}_2'(w_2)\big)\| \tag{48}$$

Observing that the difference between any entries of $\text{sgn}(w_1)$ and $\mathcal{T}_2'(w_2)$ cannot be larger than 2 in magnitude, we get

$$\begin{aligned}\|g^{\text{lasso}}(w_1) - g^{\text{lasso}'}(w_2)\| &\leq \|R_h\|\|w_1 - w_2\| + 2\delta\|\mathbb{1}\| \\ &= \|R_h\|\|w_1 - w_2\| + 2\delta M^{1/2},\end{aligned} \tag{49}$$

where $\mathbb{1}$ is the column vector with all its entries equal to one. We again arrive at a relation of the same form as (28) with parameters $c = \|R_h\|$ and $d = 2\delta M^{1/2}$. □

4. Performance Analysis: Single Agent Case

We now carry out a detailed mean-square-error analysis of the stability and performance of the stochastic sub-gradient recursion (6) in the presence of gradient noise and for *constant* step-size adaptation.

4.1 Continuous Adaptation

Since the step-size is assumed to remain constant, the effect of gradient noise is continually present and does not die out, as would occur if we were using instead a diminishing step-size, say, of the form $\mu(i) = \tau/i$. Such diminishing step-sizes annihilate the gradient noise term asymptotically albeit at the expense of turning off adaptation in the long run. In that case, the learning algorithm will lose its tracking ability. In contrast, a constant step-size keeps adaptation alive and endows the learning algorithm with a tracking mechanism and, as the analysis will show, enables convergence towards the steady-state regime at an exponential rate, $O(\alpha^i)$, for some $\alpha \in (0,1)$.

4.2 A Useful Bound

In preparation for the analysis, we first conclude from (28) that the following useful condition also holds, involving squared-norms as opposed to the actual norms:

$$\|g(w_1) - g'(w_2)\|^2 \leq e^2\|w_1 - w_2\|^2 + f^2 \quad \forall w_1, w_2, \;\; g, g' \in \partial J, \tag{50}$$

for some nonnegative constants, e^2, f^2. Indeed, if we square both sides of (28) we get

$$\begin{aligned}\|g(w_1) - g'(w_2)\|^2 \leq\; & c^2\|w_1 - w_2\|^2 + 2cd\|w_1 - w_2\| + d^2 \\ \overset{(a)}{\leq}\; & \left(c^2 + \frac{2cd}{R}\right)\|w_1 - w_2\|^2 + d^2 + 2cdR,\end{aligned} \tag{51}$$

where the constant R is any positive number that we are free to choose, and step (a) is because

$$\|w_1 - w_2\| \leq \begin{cases} R, & \text{if } \|w_1 - w_2\| < R \\ \|w_1 - w_2\|^2/R, & \text{if } \|w_1 - w_2\| \geq R \end{cases}. \tag{52}$$

It follows that the constants $\{e^2, f^2\}$ in (50) can be taken as

$$e^2 \triangleq c^2 + \frac{2cd}{R} \geq 0 \tag{53}$$

$$f^2 \triangleq d^2 + 2cdR \geq 0. \tag{54}$$

There is a second easier derivation for a bound of the form (50) without the need to introduce the parameter R but it generally leads to a looser bound. For example, observe that by squaring and appealing to Jensen's inequality we get:

$$\|g(w_1) - g'(w_2)\|^2 \leq \Big(c\|w_1 - w_2\| + d\Big)^2 \tag{55}$$

$$\leq 2c^2\|w_1 - w_2\|^2 + 2d^2. \tag{56}$$

In this case, we would select $e^2 = 2c^2$ and $f^2 = 2d^2$. We continue with (51).

4.3 Stability and Convergence

We are now ready to establish the following important conclusion regarding the stability and performance of the stochastic sub-gradient algorithm (6); the conclusion indicates that the algorithm is stable and converges exponentially fast for sufficiently small step-sizes. But first, we explain our notation and the definition of a "best" iterate, denoted by $\boldsymbol{w}_i^{\rm best}$(Nesterov, 2004). This variable is useful in the context of sub-gradient implementations because it is known that (negative) sub-gradient directions do not necessarily correspond to real descent directions (as is the case with actual gradient vectors for differentiable functions).

At every iteration i, the risk value that corresponds to the iterate $\boldsymbol{w}_i$ is $J(\boldsymbol{w}_i)$. This value is obviously a random variable due to the randomness in the data used to run the algorithm. We denote the mean risk value by $\mathbb{E}\,J(\boldsymbol{w}_i)$. The next theorem examines how fast and how close this mean value approaches the optimal value, $J(w^\star)$. To do so, the statement in the theorem relies on the *best pocket* iterate, denoted by $\boldsymbol{w}_i^{\rm best}$, and which is defined as follows. At any iteration i, the value that is saved in this pocket variable is the iterate, $\boldsymbol{w}_j$, that has generated the smallest mean risk value up to that point in time, i.e.,

$$\boldsymbol{w}_i^{\rm best} \triangleq \mathop{\arg\min}_{0\leq j\leq i} \ \mathbb{E}\ J(\boldsymbol{w}_j). \tag{57}$$

The statement below then proves that $\mathbb{E}\,J(\boldsymbol{w}_i^{\rm best})$ approaches a small neighborhood of size $O(\mu)$ around $J(w^\star)$ exponentially fast:

$$\lim_{i\to\infty} \ \mathbb{E}\ J(\boldsymbol{w}_i^{\rm best}) \ \leq \ J(w^\star) \ + \ O(\mu), \tag{58}$$

where the big-O notation $O(\mu)$ means in the order of μ.

Theorem 1 (Single agent performance) *Consider using the stochastic sub-gradient algorithm (6) to seek the unique minimizer, $w^\star$, of the optimization problem (1), where the*

risk function, $J(w)$, is assumed to satisfy Assumptions 1–3. If the step-size parameter satisfies (i.e., if it is small enough):

$$\mu < \frac{\eta}{e^2+\beta^2}, \tag{59}$$

then it holds that

$$\mathbb{E}\, J(\boldsymbol{w}_i^{\rm best}) - J(w^\star) \;\le\; \xi\cdot\alpha^i \mathbb{E}\left\|\boldsymbol{w}_0 - w^\star\right\|^2 + \mu(f^2+\sigma^2)/2, \quad \forall\, i\ge 0 \tag{60}$$

That is the convergence of $\mathbb{E}\, J(\boldsymbol{w}_i^{\rm best})$ towards the $O(\mu)-$neighborhood around $J(w^\star)$ occurs at linear rate, $O(\alpha^i)$, dictated by the parameter

$$\alpha \;\stackrel{\Delta}{=}\; 1-\mu\eta+\mu^2(e^2+\beta^2) = 1-O(\mu) \tag{61}$$

Condition (59) ensures $\alpha\in(0,1)$. In the limit:

$$\lim_{i\to\infty} \mathbb{E}\, J(\boldsymbol{w}_i^{\rm best}) - J(w^\star) \;\le\; \mu(f^2+\sigma^2)/2. \tag{62}$$

That is, for large i, $\mathbb{E}\, J(\boldsymbol{w}_i^{\rm best})$ is approximately $\mu(f^2+\sigma^2)/2$-suboptimal.

Proof : We introduce the error vector, $\widetilde{\boldsymbol{w}}_i = w^\star - \boldsymbol{w}_i$, and use it to deduce from (6)–(7) the following error recursion:

$$\widetilde{\boldsymbol{w}}_i = \widetilde{\boldsymbol{w}}_{i-1} + \mu g(\boldsymbol{w}_{i-1}) + \mu s_i(\boldsymbol{w}_{i-1}). \tag{63}$$

Squaring both sides and computing the conditional expectation we obtain:

$$\begin{aligned}\mathbb{E}\,[\|\widetilde{\boldsymbol{w}}_i\|^2 \,|\, \boldsymbol{\mathcal{F}}_{i-1}\,] &= \mathbb{E}\,[\,\|\widetilde{\boldsymbol{w}}_{i-1} + \mu g(\boldsymbol{w}_{i-1}) + \mu \boldsymbol{s}_i(\boldsymbol{w}_{i-1})\|^2 \,|\, \boldsymbol{\mathcal{F}}_{i-1}\,] \\ &\stackrel{(a)}{=} \|\widetilde{\boldsymbol{w}}_{i-1} + \mu g(\boldsymbol{w}_{i-1})\|^2 \;+\; \mu^2\mathbb{E}\,[\|\boldsymbol{s}_i(\boldsymbol{w}_{i-1})\|^2 \,|\, \boldsymbol{\mathcal{F}}_{i-1}\,] \\ &= \|\widetilde{\boldsymbol{w}}_{i-1}\|^2 + 2\mu g(\boldsymbol{w}_{i-1})^{\mathsf{T}}\widetilde{\boldsymbol{w}}_{i-1} + \mu^2\|g(\boldsymbol{w}_{i-1})\|^2 + \mu^2\mathbb{E}\,[\|\boldsymbol{s}_i(\boldsymbol{w}_{i-1})\|^2 \,|\, \boldsymbol{\mathcal{F}}_{i-1}\,].\end{aligned} \tag{64}$$

In step (a), we eliminated the cross term because, conditioned on $\boldsymbol{\mathcal{F}}_{i-1}$, the gradient noise process has zero-mean. Now, from the strong convexity condition (27), it holds that

$$g(\boldsymbol{w}_{i-1})^{\mathsf{T}}\widetilde{\boldsymbol{w}}_{i-1} \le J(w^\star) - J(\boldsymbol{w}_{i-1}) - \frac{\eta}{2}\|\widetilde{\boldsymbol{w}}_{i-1}\|^2. \tag{65}$$

Substituting into (64) gives

$$\begin{aligned}\mathbb{E}\,[\|\widetilde{\boldsymbol{w}}_i\|^2 \,|\, \boldsymbol{\mathcal{F}}_{i-1}\,] \le \|\widetilde{\boldsymbol{w}}_{i-1}\|^2 + 2\mu\left(J(w^\star) - J(\boldsymbol{w}_{i-1}) - \frac{\eta}{2}\|\widetilde{\boldsymbol{w}}_{i-1}\|^2\right) + \\ \mu^2\|g(\boldsymbol{w}_{i-1})\|^2 + \mu^2\mathbb{E}\,[\|s_i(\boldsymbol{w}_{i-1})\|^2 \,|\, \boldsymbol{\mathcal{F}}_{i-1}\,].\end{aligned} \tag{66}$$

Referring to (50), if we set $w_1 = \boldsymbol{w}_{i-1}$, $w_2 = w^\star$, and use the fact that there exists one particular sub-gradient $g'(w)$ satisfying $g'(w^\star) = 0$, we obtain:

$$\|g(\boldsymbol{w}_{i-1})\|^2 \le e^2\|\widetilde{\boldsymbol{w}}_{i-1}\|^2 + f^2. \tag{67}$$

Substituting into (66), we get

$$\begin{aligned}
&\mathbb{E}\,[\|\widetilde{\boldsymbol{w}}_i\|^2\,|\,\boldsymbol{\mathcal{F}}_{i-1}\,] \\
&\quad\leq (1-\mu\eta+\mu^2e^2)\|\widetilde{\boldsymbol{w}}_{i-1}\|^2+2\mu J(w^\star)-2\mu J(\boldsymbol{w}_{i-1})+\mu^2f^2+\mu^2\mathbb{E}\,[\|s_i(\boldsymbol{w}_{i-1})\|^2\,|\,\boldsymbol{\mathcal{F}}_{i-1}\,] \\
&\overset{(24)}{\leq}\ (1-\mu\eta+\mu^2(e^2+\beta^2))\|\widetilde{\boldsymbol{w}}_{i-1}\|^2+2\mu J(w^\star)-2\mu J(\boldsymbol{w}_{i-1})+\mu^2f^2+\mu^2\sigma^2. \qquad (68)
\end{aligned}$$

Taking expectation again we eliminate the conditioning on $\boldsymbol{\mathcal{F}}_{i-1}$ and arrive at:

$$2\mu(\mathbb{E}\,J(\boldsymbol{w}_{i-1})-J(w^\star))\ \leq\ (1-\mu\eta+\mu^2(e^2+\beta^2))\mathbb{E}\,\|\widetilde{\boldsymbol{w}}_{i-1}\|^2-\mathbb{E}\,\|\widetilde{\boldsymbol{w}}_i\|^2+\mu^2(f^2+\sigma^2). \quad (69)$$

To proceed, we simplify the notation and introduce the scalars

$$\begin{aligned}
a(i) &\triangleq \mathbb{E}\,J(\boldsymbol{w}_{i-1})-J(w^\star) && (70)\\
b(i) &\triangleq \mathbb{E}\,\|\widetilde{\boldsymbol{w}}_i\|^2 && (71)\\
\alpha &\triangleq 1-\mu\eta+\mu^2(e^2+\beta^2) && (72)\\
\tau^2 &\triangleq f^2+\sigma^2 && (73)
\end{aligned}$$

Note that since $w^\star$ is the unique global minimizer of $J(w)$, then it holds that $J(\boldsymbol{w}_{i-1})\geq J(w^\star)$ so that $a(i)\geq 0$ for all i. The variable $a(i)$ represents the average *excess risk*. Now, we can rewrite (69) more compactly as

$$2\mu a(i)\leq \alpha b(i-1)-b(i)+\mu^2\tau^2. \quad (74)$$

Iterating over $1\leq i\leq L$, gives

$$\sum_{i=1}^{L}\alpha^{L-i}(2\mu a(i)-\mu^2\tau^2)\ \ \leq\ \ \alpha^Lb(0)-b(L)\ \leq\ \alpha^Lb(0). \quad (75)$$

Let us verify that $\alpha\in(0,1)$. First, observe from expression (72) for α that $\alpha(\mu)$ is a quadratic function in μ. This function attains its minimum at location $\mu^o=\eta/(2e^2+2\beta^2)$. For any μ, the value of $\alpha(\mu)$ is larger than the minimum value of the function at μ^o, i.e., it holds that

$$\alpha\geq 1-\frac{\eta^2}{4(e^2+\beta^2)}. \quad (76)$$

Now, comparing relations (34) and (28), we find that the sub-gradient vector satisfies:

$$\eta\|w-w^\star\|\leq\|g(w)\|\leq c\|w-w^\star\|+d,\quad\forall w, \quad (77)$$

which implies that $\eta\leq c$ since the above inequality must hold for all w. It then follows from (53) that $e^2>\eta^2$ and from (76) that

$$\alpha\geq 1-\frac{\eta^2}{4\eta^2}>0. \quad (78)$$

In other words, the parameter α is positive. Furthermore, some straightforward algebra using (72) shows that condition (59) implies $\alpha<1$. We therefore established that $\alpha\in(0,1)$, as desired.

Returning to (74), we note that because the (negative) sub-gradient direction is not necessarily a descent direction, we cannot ensure that $a(i) < a(i-1)$. However, we can still arrive at a useful conclusion by introducing a pocket variable, denoted by $a^{\rm best}(L) \geq 0$. This variable saves the value of the smallest increment, $a(j)$, up to time L, i.e.,

$$a^{\rm best}(L) \stackrel{\Delta}{=} \min_{1 \leq i \leq L} a(i) \; . \tag{79}$$

Let further $\boldsymbol{w}_L^{\rm best}$ denote the corresponding iterate $\boldsymbol{w}_i$ where this best value is achieved. Replacing $a(i)$ by $a^{\rm best}(L)$ in (75) gives

$$\begin{aligned} (2\mu a^{\rm best}(L) - \mu^2\tau^2) &\leq \alpha^L b(0) \left(\sum_{i=1}^{L} \alpha^{L-i} \right)^{-1} \\ &= \alpha^L b(0) \left(\frac{1-\alpha^L}{1-\alpha} \right)^{-1} \\ &= b(0) \cdot \frac{\alpha^L(1-\alpha)}{1-\alpha^L}, \end{aligned} \tag{80}$$

or, equivalently,

$$2\mu a^{\rm best}(L) \; \leq \; \mu^2\tau^2 \; + \; b(0) \cdot \frac{\alpha^L(1-\alpha)}{1-\alpha^L}. \tag{81}$$

Plugging the definition of $a^{\rm best}(L)$ and $b(0)$, we will arrive at

$$\mathbb{E}\, J(\boldsymbol{w}_L^{\rm best}) - J(w^\star) \leq \alpha^L \frac{(1-\alpha)}{2\mu(1-\alpha^L)} \mathbb{E}\, \|\boldsymbol{w}_0 - w^\star\|^2 + \mu(f^2+\sigma^2)/2 \tag{82}$$

Taking the limit as $L \to \infty$, we conclude that

$$\lim_{L \to \infty} \mathbb{E}\, J(\boldsymbol{w}_L^{\rm best}) - J(w^\star) \leq \mu\tau^2/2 = \mu(f^2+\sigma^2)/2. \tag{83}$$

■

Remark #1: It is important to note that result (50) extends and enhances a useful result derived by (Agarwal et al., 2012) where the following *lower bound* was established (using our notation):

$$\mathbb{E}\, J(w_i) - J(w^\star) \geq \frac{\zeta_1}{i} \left[\mathbb{E}\, \|w_0 - w^\star\|^2 \right] \tag{84}$$

for some constant $\zeta_1 > 0$. This result shows that the convergence of $J(w_i)$ towards $J(w^\star)$ cannot be better than a linear rate when one desires convergence towards the exact minimum value. In contrast, our analysis that led to (50) establishes the following *upper bound*:

$$\mathbb{E}\, J(w_i) - J(w^\star) \leq \zeta \alpha^i \left[\mathbb{E}\, \|w_0 - w^\star\|^2 \right] \; + \; O(\mu) \tag{85}$$

for some constant $\zeta > 0$. Observe that this expression is showing that $J(w_i)$ can actually approach a small $O(\mu)-$neighborhood around $J(w_i)$ *exponentially fast* at a rate that is dictated by the scalar $0 < \alpha < 1$. It is clear that the two results (84) and (85) on the convergence rate do not contradict each other. On the contrary, they provide complementary

views on the convergence behavior (from below and from above). Still, it is useful to remark that the analysis employed by Agarwal and Bartlett (2012) imposes a stronger condition on the risk function than our condition: they require the risk function to be Lipschitz continuous. In comparison, we require the subgradient (and not the risk function) to be affine Lipschitz, which makes the current results applicable to a borader class of problems. ■

Remark #2: We can similarly comment on how our result (60) relates to the useful results that appear in (Nedic, 2002). Using our notation, the main conclusion that follows from propositions 3.2 and 3.3 in this work in this work is that

$$\mathbb{E}\, J(w_i^{\rm best}) - J(w^\star) \leq \frac{\zeta_2}{i}\mathbb{E}\,\|w_0 - w^\star\|^2 + O(\mu) \tag{86}$$

for some constant $\zeta_2 > 0$. This result only ensures a sub-linear rate of convergence. In contrast, our convergence analysis leads to the following result

$$\mathbb{E}\, J(w_i^{\rm best}) - J(w^\star) \leq \zeta\alpha^i \left[\mathbb{E}\,\|w_0 - w^\star\|^2\right] \;+\; O(\mu) \tag{87}$$

for some scalar $0 < \alpha < 1$, which shows that convergence actually occurs at a linear rate. This conclusion is clearly more powerful. Furthermore, as was the case with the treatment in (Agarwal et al., 2012), the result (86) is derived in (Nedic, 2002) by assuming the sub-gradient vectors are bounded, which is a stronger condition than the affine Lipschitz condition used in the current manuscript.

■

The above theorem only clarifies the performance of the best pocket value, which is not readily available during the algorithm implementation since the risk function itself cannot be evaluated. That is, $J(\boldsymbol{w}_i)$ cannot be computed because $J(w)$ is not known due to the lack of knowledge about the probability distribution of the data. However, a more practical conclusion can be deduced from the statement of the theorem as follows. Introduce the geometric sum:

$$S_L \;\triangleq\; \sum_{j=1}^{L} \alpha^{L-j} \;=\; \frac{1-\alpha^L}{1-\alpha}, \tag{88}$$

as well as the normalized and convex-combination coefficients:

$$r_L(j) \;\triangleq\; \frac{\alpha^{L-j}}{S_L}, \quad j = 1, 2, \ldots, L. \tag{89}$$

Using these coefficients, we define the weighted iterate

$$\bar{\boldsymbol{w}}_L \;\triangleq\; \sum_{j=1}^{L} r_L(j)\boldsymbol{w}_j = \frac{1}{S_L}\left[\alpha^{L-1}\boldsymbol{w}_1 + \alpha^{L-2}\boldsymbol{w}_2 + \ldots + \alpha\boldsymbol{w}_{L-1} + \boldsymbol{w}_L\right]. \tag{90}$$

Observe that, in contrast to $\boldsymbol{w}_L^{\rm best}$, the above weighted iterate is computable since its value depends on the successive iterates $\{\boldsymbol{w}_j\}$ and these are available during the operation of the algorithm. Observe further that $\bar{\boldsymbol{w}}_L$ satisfies the recursive construction:

$$\bar{\boldsymbol{w}}_L \;=\; \left(1 - \frac{1}{S_L}\right)\bar{\boldsymbol{w}}_{L-1} \;+\; \frac{1}{S_L}\boldsymbol{w}_L. \tag{91}$$

In particular, as $L \to \infty$, we have $S_L \to 1/(1-\alpha)$, and the above recursion simplifies in the limit to

$$\bar{\boldsymbol{w}}_L \;=\; \alpha\bar{\boldsymbol{w}}_{L-1} \;+\; (1-\alpha)\boldsymbol{w}_L. \tag{92}$$

Now, since $J(\cdot)$ is a convex function, it holds that

$$J(\bar{\boldsymbol{w}}_L) \;=\; J\left(\sum_{j=1}^{L} r_L(j)\boldsymbol{w}_j\right) \;\leq\; \sum_{j=1}^{L} r_L(j)J(\boldsymbol{w}_j). \tag{93}$$

Using this fact, the following corollary derives a result similar to (62) albeit applied to $\bar{\boldsymbol{w}}_L$.

Corollary 2 (Weighted iterate) *Under the same conditions as in Theorem 1, it holds that*

$$\lim_{L\to\infty} \mathbb{E}\, J(\bar{\boldsymbol{w}}_L) - J(w^\star) \leq \mu(f^2+\sigma^2)/2, \tag{94}$$

and the convergence of $\mathbb{E}\, J(\bar{\boldsymbol{w}}_L)$ *towards* $J(w^\star)$ *continues to occur at the same exponential rate,* $O(\alpha^L)$.

Proof : We start from (75), namely,

$$\sum_{i=1}^{L} \alpha^{L-i}(2\mu\mathbb{E}\, J(\boldsymbol{w}_i) - 2\mu J(w^\star) - \mu^2\tau^2) \leq \alpha^L b(0), \tag{95}$$

and divide both sides by the same sum:

$$\sum_{i=1}^{L} \left(\frac{\alpha^{L-i}}{\sum_{j=1}^{L}\alpha^{L-j}}\right)(2\mu\mathbb{E}\, J(\boldsymbol{w}_i) - 2\mu J(w^\star) - \mu^2\tau^2) \leq \left(\frac{\alpha^L}{\sum_{j=1}^{L}\alpha^{L-j}}\right) b(0), \tag{96}$$

which gives

$$\sum_{i=1}^{L} r(i)(2\mu\mathbb{E}\, J(\boldsymbol{w}_i) - 2\mu J(w^\star)) \leq \frac{\alpha^L(1-\alpha)}{1-\alpha^L} b(0) \;+\; \mu^2\tau^2. \tag{97}$$

Appealing to the convexity property (93) we conclude that

$$2\mu(\mathbb{E}\, J(\bar{\boldsymbol{w}}_L) - 2\mu J(w^\star)) \leq \frac{\alpha^L(1-\alpha)}{1-\alpha^L} b(0) \;+\; \mu^2\tau^2. \tag{98}$$

Taking the limit as $L \to \infty$ leads to (94). ■

Using α as a scaling weight in (90) may still be inconvenient because its value needs to be determined. The analysis however suggests that we may replace α by any parameter κ satisfying $\alpha \leq \kappa \leq 1$. The parameter κ plays a role similar to the step-size, μ: both become parameters selected by the designer. Next, we introduce the new weighted variable:

$$\bar{\boldsymbol{w}}'_L \;\stackrel{\Delta}{=}\; \sum_{j=1}^{L} r'_L(j)\boldsymbol{w}_j, \tag{99}$$

where now

$$r'_L(j) = \kappa^{L-j}/S'_L, \;\; j = 1, 2, \ldots, L, \tag{100}$$

and

$$S'_L = \sum_{j=1}^{L} \kappa^{L-j}. \tag{101}$$

Corollary 3 (Relaxed Weighted iterate) *Under the same conditions as in Theorem 1 and $\alpha \leq \kappa < 1$, relation (94) continues to hold with $\bar{\boldsymbol{w}}_L$ replaced by $\bar{\boldsymbol{w}}'_L$. Moreover, convergence now occurs at the exponential rate $O(\kappa^L)$.*

Proof : The argument requires some modification relative to what we have done before. We start from (74) again:

$$2\mu a(i) \leq \alpha b(i-1) - b(i) + \mu^2\tau^2. \tag{102}$$

But unlike the previous derivation in (75), now we use κ to expand the recursion from iteration $i = 1$ to L:

$$\begin{aligned}
\sum_{i=1}^{L} \kappa^{L-i}(2\mu a(i) - \mu^2\tau^2) &\leq \sum_{i=1}^{L} \kappa^{L-i}\Big(\alpha b(i-1) - b(i)\Big) \\
&= \sum_{i=0}^{L-1} \kappa^{L-i-1}\alpha b(i) - \sum_{i=1}^{L} \kappa^{L-i} b(i) \\
&= \sum_{i=0}^{L-1} \kappa^{L-i-1}(\alpha - \kappa) b(i) + \kappa^{L-1}\alpha b(0) - b(L) \\
&\leq \kappa^L b(0),
\end{aligned} \tag{103}$$

where in the last inequality we used the fact that $\kappa \geq \alpha$. We can now proceed from here and complete the argument as before. ■

Corollary 4 (Mean-Square-Deivation Performance) *Under the same conditions as in Theorem 1 and $\alpha \leq \kappa < 1$. It holds that*

$$\lim_{L\to\infty} \mathbb{E}\,\|\bar{\boldsymbol{w}}'_L - w^\star\|^2 \leq \mu(f^2 + \sigma^2)/\eta \tag{104}$$

Moreover, convergence to the steady-state regime occurs at the exponential rate $O(\kappa^L)$.

Proof : Referring to equation (31), we get

$$\mathbb{E}\,\|\bar{\boldsymbol{w}}'_i - w^\star\|^2 \leq \frac{2}{\eta}\left(\mathbb{E}\,J(\bar{\boldsymbol{w}}'_i) - J(w^\star)\right) \tag{105}$$

Combining with the corollary 3, we arrive at (104). ■

It is interesting to compare result (94) with what happens in the case of *differentiable* risk functions. In that case, the standard stochastic gradient algorithm, using the actual gradient vector rather than sub-gradients, can be employed to seek the minimizer, $w^\star$. It was established in (Sayed, 2014a, Ch. 4) that for risk functions that are twice-differentiable, the stochastic gradient algorithm guarantees

$$\lim_{L\to\infty} \mathbb{E}\, J(\boldsymbol{w}_L) - J(w^\star) = \frac{\mu}{4}\sigma^2, \tag{106}$$

where the right-hand side is dependent on σ^2 alone; this factor arises from the bound (24) on the gradient noise process. In contrast, in the non-smooth case (94), we established here a similar bound that is still in the order of $O(\mu)$. However, the size of the bound is not solely dependent on σ^2 anymore but it also includes the factor f^2; this latter factor arises from condition (50) on the sub-gradient vectors. That is, there is some minor degradation (since μ is small) that arises from the non-smoothness of the risk function. If we set $f = 0$ in (94), we recover (106) up to a scaling factor of 2. Although the bound in this case is still $O(\mu)$, as desired, the reason why it is not as tight as the bound derived in the smooth case in (Sayed, 2014a) is because the derivation in the current paper is not requiring the risk function to be twice differentiable, as was the case in (Sayed, 2014a), and we are also discarding the term $b(L)$ in equation (75). The important conclusion to note is that the right-hand side of (94) is also $O(\mu)$, as in the smooth case (106).

4.4 Interpretation of Results

The results derived in this section highlight several important facts that we would like to summarize:

(1) First, it has been observed in the optimization literature that sub-gradient descent iterations can perform poorly in *deterministic* problems (where $J(w)$ is known). Their convergence rate is $O(1/\sqrt{i})$ under convexity and $O(1/i)$ under strong-convexity (Nesterov, 2004) when decaying step-sizes, $\mu(i) = 1/i$, are used to ensure convergence (Shalev-Shwartz et al., 2011). Our arguments show that the situation is different in the context of *stochastic* optimization when true sub-gradients are approximated from streaming data. By using *constant* step-sizes to enable continuous learning and adaptation, the sub-gradient iteration is now able to achieve exponential convergence at the rate of $O(\alpha^i)$ for some $\alpha = 1 - O(\mu)$.

(2) Second, of course, this substantial improvement in convergence rate comes at a cost, but one that is acceptable and controllable. Specifically, we cannot guarantee convergence of the algorithm to the global minimum value, $J(w^\star)$, anymore but can instead approach this optimal value with high accuracy in the order of $O(\mu)$, where the size of μ is under the designer's control and can be selected as small as desired.

(3) Third, this performance level is sufficient in most cases of interest because, in practice, one rarely has an infinite amount of data and, moreover, the data is often subject to distortions not captured by any assumed models. It is increasingly recognized in the literature that it is not always necessary to ensure exact convergence towards the

optimal solution, $w^\star$, or the minimum value, $J(w^\star)$, because these optimal values may not reflect accurately the true state due to modeling error. For example, it is explained in the works (Bousquet and Bottou, 2008; Bottou, 2012, 2010) that it is generally unnecessary to reduce the error measures below the statistical error level that is present in the data.

5. Applications: Single Agent Case

We now apply the results of the previous analysis to several cases in order to illustrate that *stochastic* sub-gradient constructions can indeed lead to good performance.

Example 5 (LASSO problem). For the LASSO problem, we choose $R = 0.5$ so that

$$f^2 = d^2 + cd = 4\delta^2 M + 2\delta M^{\frac{1}{2}}. \tag{107}$$

It then follows that

$$\lim_{L\to\infty} \mathbb{E}\, J^{\text{lasso}}(\bar{\boldsymbol{w}}_L) - J^{\text{lasso}}(w^\star) \leq \mu(2\delta^2 M + \delta M^{\frac{1}{2}}) + \frac{\mu}{2}\sigma_n^2 \text{Tr}(R_h). \tag{108}$$

In order to verify this result, we run a simulation with $\mu = 0.001$, $\delta = 0.002$, and $M = 100$. Only two entries in w° are assumed to be nonzero. The regression vectors and noise process $\{\boldsymbol{h}_i, \boldsymbol{n}(i)\}$ are both generated according to zero-mean normal distributions with variances $R_h = I$ and $\sigma_n^2 = 0.01$, respectively. From the optimality condition, $0 \in \partial J(\boldsymbol{w}^\star)$, it is easy to conclude that(Donoho and Johnstone, 1994)

$$w^\star = \mathcal{S}_\delta(w^\circ), \tag{109}$$

where the symbol $\mathcal{S}_\delta$ represents the soft-thresholding function with parameter δ, i.e.,

$$\mathcal{S}_\delta(x) = \text{sgn}(x) \cdot \max\{0, |x| - \delta\}. \tag{110}$$

Figure 1 plots the evolution of the excess-risk curve, $\mathbb{E}\, J^{\text{lasso}}(\bar{\boldsymbol{w}}_L) - J^{\text{lasso}}(w^\star)$, obtained by averaging over 50 experiments. The figure compares the performance of the standard LMS solution:

$$\boldsymbol{w}_i = \boldsymbol{w}_{i-1} + \mu \boldsymbol{h}_i(\boldsymbol{\gamma}(i) - \boldsymbol{h}_i^{\mathsf{T}} \boldsymbol{w}_{i-1}), \tag{111}$$

against the sparse sub-gradient version(Duttweiler, 2000; Kopsinis et al., 2011; Chen et al., 2009):

$$\boldsymbol{w}_i = \boldsymbol{w}_{i-1} + \mu \boldsymbol{h}_i(\boldsymbol{\gamma}(i) - \boldsymbol{h}_i^{\mathsf{T}} \boldsymbol{w}_{i-1}) - \mu\delta \cdot \text{sgn}(\boldsymbol{w}_{i-1}). \tag{112}$$

It is observed that the stochastic sub-gradient implementation satisfies the bound predicted by theory.

□

Example 6 (SVM problem). For the SVM problem, we again select $R = 0.5$ and conclude that

$$\lim_{L\to\infty} \mathbb{E}\, J^{\text{svm}}(\bar{\boldsymbol{w}}_L) - J^{\text{svm}}(w^\star) \leq \frac{\mu}{2}\left(5\text{Tr}(R_h) + 2\rho(\text{Tr}(R_h))^{\frac{1}{2}}\right). \tag{113}$$

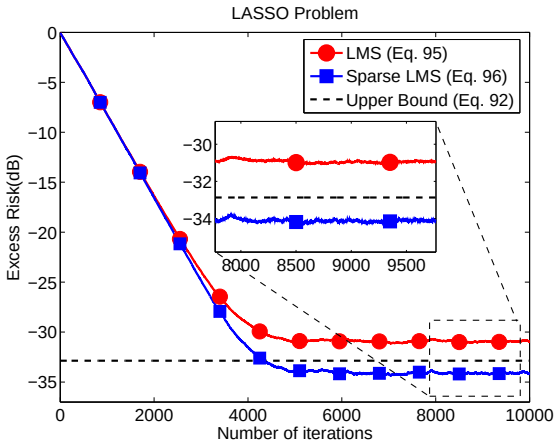

Figure 1: LASSO problem. The excess-risk curves, i.e. $\big(\mathbb{E}\, J(\boldsymbol{w}_L) - J(w^\star)\big)$, for LMS and for LASSO-LMS are obtained by averaging over 50 experiments.

Actually, for the SVM construction, we can obtain a tighter upper bound than the one provided by Corollary 2; this is because we can exploit the special structure of the SVM cost to arrive at

$$\lim_{L\to\infty} \mathbb{E}\, J^{\rm svm}(\bar{\boldsymbol{w}}_L) - J^{\rm svm}(w^\star) \leq \mu\big(\rho^2\|w^\star\|^2 + \rho + {\rm Tr}(R_h)/2\big), \tag{114}$$

with convergence rate $\alpha = 1 - 2\mu\rho + \mu^2\rho^2$. The proof is provided in Appendix A. We compare the performance of the stochastic sub-gradient SVM implementation:

$$\begin{cases} \boldsymbol{w}_i = (1-\rho\mu)\boldsymbol{w}_{i-1} - \mu\boldsymbol{\gamma}(i)\boldsymbol{h}_i\mathbb{I}[\boldsymbol{\gamma}(i)\boldsymbol{h}_i^{\mathsf{T}}\boldsymbol{w}_{i-1} \leq 1] \\ S_i = (1-2\mu\rho+\mu^2\rho^2)S_{i-1} + 1 \\ \bar{\boldsymbol{w}}_i = \left(1 - \dfrac{1}{S_i}\right)\bar{\boldsymbol{w}}_{i-1} \;+\; \dfrac{1}{S_i}\boldsymbol{w}_i \end{cases}, \tag{115}$$

(with all variables initiate at zero) against LIBSVM (a popular SVM solver that uses dual quadratic programming) (Chang and Lin, 2011). The test data is obtained from the LIBSVM website[2] and also from the UCI dataset[3]. We first use the Adult dataset after preprocessing (Platt, 1999) with 11,220 training data and 21,341 testing data in 123 feature dimensions. To ensure a fair comparison, we use linear LIBSVM with the exact same parameters as the sub-gradient method. Hence, we choose $C = 5 \times 10^2$ for LIBSVM, which corresponds to $\rho = \frac{1}{C} = 2 \times 10^{-3}$. We also set $\mu = 0.05$.

We can see from Fig. 2 that the stochastic sub-gradient algorithm is able converge to the performance of LIBSVM quickly. Since we only use each data point once, and since each iteration is computationally simpler, the sub-gradient implementation ends up being

2. `http://www.csie.ntu.edu.tw/~cjlin/libsvmtools/datasets/binary.html`
3. `http://archive.ics.uci.edu/ml/`

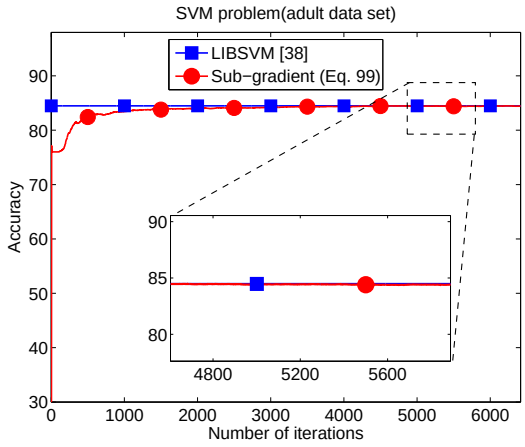

Figure 2: SVM solvers applied to the Adult data set. Comparison of the performance accuracy, percentage of correct prediction over test dataset, for LIBSVM(Chang and Lin, 2011) and a stochastic sub-gradient implementation (115).

computationally more efficient. We also examine the performance of the sub-gradient SVM solver on another large-scale dataset, namely, the Reuters Corpus Volume I (RCV1) data with 20242 training data and 253843 testing data consisting of 47236 feature dimensions. The chosen parameters are $C = 1 \times 10^5, \mu = 0.2$. The performance is shown in Fig. 3.

□

Example 7 (Image denoising problem). We next illustrate how the stochastic sub-gradient implementation can match the performance of some sophisticated techniques for image denoising, such as the FISTA algorithm. This latter technique solves the denoising problem by relying on the use of proximal projections and acceleration methods applied to a dual problem (Beck and Teboulle, 2009a,b).

One classical formulation for the image denoising problem with total-variation regularization involves seeking an image (or matrix) that minimizes the following deterministic cost(Rudin et al., 1992):

$$\min_{\mathcal{I}} \ \frac{1}{2}\|\mathcal{I} - \mathcal{I}_{\text{noisy}}\|_F^2 + \lambda \cdot \text{TV}(\mathcal{I}), \tag{116}$$

where $\lambda > 0$ is a regularization factor. Moreover, the term $\mathcal{I}$ denotes some rectangular or square image that we wish to recover, say, of size $N \times N$, and $\mathcal{I}_{\text{noisy}}$ refers to the available noisy measurement of the true image:

$$\mathcal{I}_{\text{noisy}} \ = \ \mathcal{I}^o \ + \ \text{noise}, \tag{117}$$

where the noise term refers to a zero-mean perturbation. The notation $\|\cdot\|_F$ denotes the Frobenious norm of its matrix argument, and the operation $\text{TV}(\cdot)$ stands for a total-variation

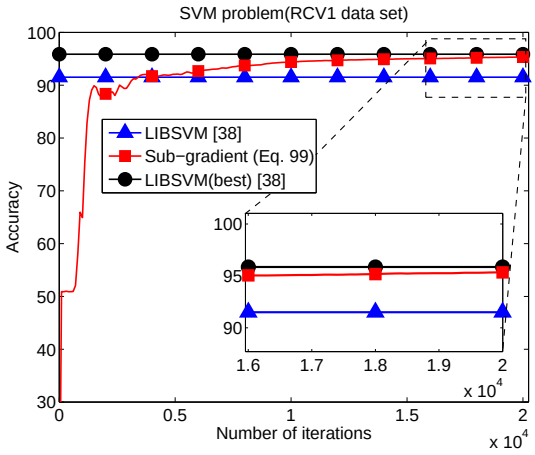

Figure 3: SVM solvers applied to the RCV1 data set. Comparison of the performance accuracy, percentage of correct prediction over test dataset, for LIBSVM(Chang and Lin, 2011) and a stochastic sub-gradient implementation (115). The blue line for LIBSVM is generated by using the same parameters as the sub-gradient implementation, while the black line is determined by using cross validation. The difference between both lines is because LIBSVM achieves higher accuracy when setting ρ to a large value, say, around the value of one. In comparison, from (114) we know that sub-gradient methods need a small ρ to achieve higher accuracy.

computation, which is defined as follows:[4]

$$\mathrm{TV}(\mathcal{I}) \triangleq \sum_{m,n} |\mathcal{I}(m,n) - \mathcal{I}(m+1,n)| + |\mathcal{I}(m,n) - \mathcal{I}(m,n+1)|. \tag{118}$$

The total variation term essentially encourages the difference between the image and some of its shifted versions to remain nearly sparse. We may also formulate a stochastic version of the denoising problem by considering instead:

$$\min_{\mathcal{I}} \ \frac{1}{2}\mathbb{E}\,\|\mathcal{I} - \boldsymbol{\mathcal{I}}_{\mathrm{noisy}}\|_F^2 + \lambda \cdot \mathrm{TV}(\mathcal{I}), \tag{119}$$

where the expectation is now over the randomness in the noise used to generate the noisy image (here we only consider the synthesis case). The sub-gradient of the Total Variation term is straightforward to compute. For illustration purposes, we evaluate the sub-gradient at some arbitrary point (m_0, n_0). Expanding the summation and separating the terms related to point (m_0, n_0), we obtain:

$$\begin{aligned}\mathrm{TV}(\mathcal{I}) \ = \ & |\mathcal{I}(m_0,n_0) - \mathcal{I}(m_0+1,n_0)| + |\mathcal{I}(m_0,n_0) - \mathcal{I}(m_0,n_0+1)| + \\ & |\mathcal{I}(m_0-1,n_0) - \mathcal{I}(m_0,n_0)| + |\mathcal{I}(m_0,n_0-1) - \mathcal{I}(m_0,n_0)| + \mathrm{rest}, \end{aligned} \tag{120}$$

4. Here, we only consider the discrete ℓ_1-based anisotropic TV and neglect the boundary modification.

	Test Image	kodim1	kodim5	kodim7	kodim8	kodim11	kodim14
PSNR(dB)	Sub-gradient	**25.19**	**25.18**	**29.43**	**24.59**	**27.80**	**30.32**
	FISTA	24.90	24.87	29.14	24.26	27.59	30.25
Time(s)	Sub-gradient	**8.88**	**9.33**	**8.50**	8.46	**9.00**	**8.7**
	FISTA	9.16	9.78	10.15	**8.22**	10.24	9.19
	Test Image	kodim15	kodim17	kodim19	kodim21	kodim23	kodim24
PSNR(dB)	Sub-gradient	**30.32**	**29.38**	**27.53**	**27.29**	**31.68**	**26.25**
	FISTA	30.25	29.17	27.23	27.03	31.51	25.95
Time(s)	Sub-gradient	**9.07**	**9.50**	9.60	**9.45**	**9.17**	8.88
	FISTA	10.13	9.98	**9.47**	9.62	10.17	**8.51**

Table 1: Comparison between the stochastic sub-gradient method (121) and FISTA(Beck and Teboulle, 2009a) over the KODIM test image set (c.f. footnote 4). All test images are subject to additive zero-mean Gaussian noise with standard variance 0.1 (with respect to image values in the range $[0, 1]$). We set $\lambda = 0.08, \mu = 0.002$ and 300 max iterations for sub-gradient methods. For different values of λ and μ, the results will be different, but the algorithms will perform similarly when μ is chosen properly. The results in the table show that the sub-gradient implementation can, in general, achieve similar or higher PSNR in shorter time.

where the *rest* variable refers to terms that do not contain the variable $\mathcal{I}(m_0, n_0)$. Computing the sub-gradient with respect to $\mathcal{I}(m_0, n_0)$ will generate four terms with the sign function as in the LASSO problem. It is then clear that stochastic sub-gradient implementation in this case is given by:

$$\boldsymbol{\mathcal{I}}_i = \boldsymbol{\mathcal{I}}_{i-1} + \mu \left(\boldsymbol{\mathcal{I}}_{i-1} - \boldsymbol{\mathcal{I}}_{\text{noisy}} + \sum_{j=1}^{4} \lambda \cdot \text{sgn}(\boldsymbol{\mathcal{I}}_{i-1} - \boldsymbol{\mathcal{I}}_{i-1}^{j}) \right), \tag{121}$$

where $\boldsymbol{\mathcal{I}}_i$ represents the recovered image at iteration i, $\boldsymbol{\mathcal{I}}_i^1$ represents shifting the image to the left by one pixel, while $\boldsymbol{\mathcal{I}}_i^2, \boldsymbol{\mathcal{I}}_i^3, \boldsymbol{\mathcal{I}}_i^4$ represent shifting the image to the right, up, and down by one pixel, respectively. We observe that recursion (121) now iterates repeatedly over the *same* single image, $\boldsymbol{\mathcal{I}}_{\text{noisy}}$. Accordingly, in this example, the stochastic gradient noise does not vary over time, i.e.,

$$s_i(\boldsymbol{\mathcal{I}}_i) \;=\; \mathcal{I}^o - \boldsymbol{\mathcal{I}}_{\text{noisy}}, \quad \forall i. \tag{122}$$

Nevertheless, Assumption 1 still holds; it was not required there that the gradient noise process cannot be independent of time. Table 5 lists performance results using the Kodak image suite[5]. The table lists two metrics. The first metric is the PSNR defined as

$$\text{PSNR} = 10 \times \log \frac{(255)^2}{\text{MSE}}, \tag{123}$$

5. `http://r0k.us/graphics/kodak/`

where MSE represents the mean-square-error, and the second metric is the execution time. For a fair comparison, we used similar un-optimized MATLAB codes[6] under the same computer environment. The table shows that the sub-gradient implementation can achieve comparable or higher PSNR values in shorter time. Clearly, if we vary the algorithm parameters, these values will change. However, in general, it was observed in these experiments that the sub-gradient implementation succeeds in matching the performance of FISTA reasonably well. □

Figure 4: Comparison of the performance of FISTA and sub-gradient implementations on test image Kodim 23 (zoom-in) under low PSNR (13dB). The result of the sub-gradient implementation is almost indistinguishable from the result of FISTA.

6. Problem Formulation: Multi-Agent Case

We now extend the previous analysis to multi-agent networks where a collection of agents cooperate with each other to seek the minimizer of an aggregate cost of the form:

$$\min_{w} \sum_{k=1}^{N} J_k(w), \tag{124}$$

where k refers to the agent index. Each individual risk function continues to be expressed as the expected value of some loss function:

$$J_k(w) \triangleq \mathbb{E}\, Q_k(w; \boldsymbol{x}_k). \tag{125}$$

The expectation is over the data at agent k. We continue to assume that the individual costs satisfy Assumptions 2 and 3, i.e., each $J_k(w)$ is strongly-convex and its sub-gradient vectors are affine-Lipschitz with parameters $\{\eta_k, c_k, d_k\}$; we are attaching a subscript k to these parameters to make them agent-dependent (alternatively, if desired, we can replace them by agent-independent parameters by using bounds on their values). We further assume that the individual risks share a common minimizer, $w^\star$, which will therefore agree with the global minimizer for (124). This scenario corresponds to the important situation in which the agents have a common objective (or task), namely, that of estimating the same parameter vector, $w^\star$, in a distributed manner through *localized* interactions and cooperation.

6. Code for FISTA is available at `http://iew3.technion.ac.il/~becka/papers/tv_fista.zip`.

6.1 Network Model

Thus, consider a network consisting of N separate agents connected by a topology. As described in (Sayed, 2014a,b), we assign a pair of nonnegative weights, $\{a_{k\ell}, a_{\ell k}\}$, to the edge connecting any two agents k and ℓ. The scalar $a_{\ell k}$ is used by agent k to scale the data it receives from agent ℓ and similarly for $a_{k\ell}$. The network is said to be *connected* if paths with nonzero scaling weights can be found linking any two distinct agents in both directions. The network is said to be *strongly–connected* if it is connected with at least one self-loop, meaning that $a_{kk} > 0$ for some agent k. Figure 5 shows one example of a strongly–connected network. For emphasis in this figure, each edge between two neighboring agents is represented by two directed arrows. The neighborhood of any agent k is denoted by $\mathcal{N}_k$ and it consists of all agents that are connected to k by edges; we assume by default that this set includes agent k regardless of whether agent k has a self-loop or not.

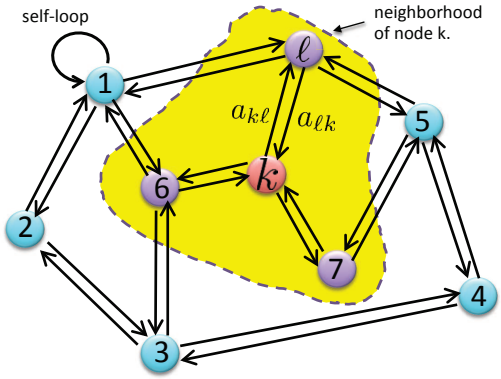

Figure 5: Agents that are linked by edges can share information. The neighborhood of agent k is marked by the broken line and consists of the set $\mathcal{N}_k = \{6, 7, \ell, k\}$.

There are several strategies that the agents can employ to seek the minimizer, $w^\star$, including consensus and diffusion strategies (Kar and Moura, 2009; Nedic and Ozdaglar, 2009; Yu et al., 2009; Sayed, 2014a,b). In this work, we focus on the latter class since diffusion implementations have been shown to have superior stability and performance properties over consensus strategies when used in the context of adaptation and learning from streaming data (i.e., when the step-sizes are set to a constant value as opposed to a diminishing value) (Sayed, 2014a,b; Tu and Sayed, 2012). As explained earlier, diminishing step-sizes annihilate the gradient noise term but disable adaptation and learning in the long run. On the other hand, constant step-size updates keep adaptation alive, which permits gradient noise to seep into the operation of the algorithm. The challenge is to show that the dynamics of the algorithm over the network is such that this noise effect does not degrade performance and that the network will still able to learn the unknown. This kind of analysis has been answered before in the affirmative for smooth twice-differentiable functions, $J_k(w)$ — see (Sayed, 2014a,b; Chen and Sayed, 2015a,b). In this work, we want to pursue the analysis more generally for possibly *non-differentiable* costs in order to encompass im-

portant applications (such as SVM learning by multi-agents or LASSO and sparsity-aware learning by similar agents(Di Lorenzo et al., 2012; Di Lorenzo and Sayed, 2013; Liu et al., 2012; Chouvardas et al., 2012)). We also want to pursue the analysis under the weaker affine-Lipschitz assumption on the sub-gradients than the stronger conditions used in the prior literature, as we already explained in the earlier sections.

6.2 Distributed Strategy

We therefore consider the following diffusion strategy in its adapt-then-combine (ATC) form:

$$\begin{cases} \boldsymbol{\psi}_{k,i} = \boldsymbol{w}_{k,i-1} - \mu\, \widehat{g}_k(\boldsymbol{w}_{k,i-1}) \\ \boldsymbol{w}_{k,i} = \displaystyle\sum_{\ell \in \mathcal{N}_k} a_{\ell k} \boldsymbol{\psi}_{\ell,i} \end{cases} . \tag{126}$$

Here, the first step involves adaptation by agent k by using a stochastic sub-gradient iteration, while the second step involves aggregation; we assume the gradient noise processes across all agents are independent of each other. The entries $A = [a_{\ell k}]$ define a left-stochastic matrix, namely, the entries of A are non-negative and each of its columns adds up to one. Since the network is strongly-connected, the combination matrix A will be primitive (Meyer, 2000; Sayed, 2014a). This implies that A will admit a Jordan-decomposition of the form:

$$A = V_\epsilon J V_\epsilon^{-1} \;\triangleq\; \left[\begin{array}{c|c} p & V_R \end{array}\right] \left[\begin{array}{c|c} 1 & 0 \\ \hline 0 & J_\epsilon \end{array}\right] \left[\begin{array}{c} \mathbb{1}^{\mathsf{T}} \\ \hline V_L^{\mathsf{T}} \end{array}\right], \tag{127}$$

with a single eigenvalue at one and all eigenvalues strictly inside the unit circle. The matrix J_ϵ has a Jordan structure with the ones that would typically appear along its first sub-diagonal replaced by a small positive number, $\epsilon > 0$. Note that the eigenvectors of A corresponding to the eigenvalue at one are denoted by

$$Ap = p, \quad A^{\mathsf{T}}\mathbb{1} = \mathbb{1}. \tag{128}$$

It is further known from the Perron-Frobenius theorem (Meyer, 2000) that the entries of p are all strictly positive and we normalize them to add up to one. We denote the individual entries of p by $\{p_k\}$:

$$p_k > 0, \quad \sum_{k=1}^{N} p_k = 1. \tag{129}$$

Furthermore, since $V_\epsilon V_\epsilon^{-1} = I$, it holds that

$$V_R^{\mathsf{T}}\mathbb{1} = 0, \quad V_L^{\mathsf{T}} p = 0, \quad V_L^{\mathsf{T}} V_R = I. \tag{130}$$

6.3 Network Performance

We are now ready to establish the following extension of Theorem 1 to the network case. The result establishes that the distributed strategy is stable and converges exponentially fast for sufficiently small step-sizes. The statement below is again in terms of a pocket variable, which we define as follows.

At every iteration i, the risk value that is attained by iterate $\boldsymbol{w}_{k,i}$ is $J_k(\boldsymbol{w}_{k,i})$. This value is a random variable due to the randomness in the streaming data used to run the algorithm. We denote the mean risk value at agent k by $\mathbb{E}\, J_k(\boldsymbol{w}_{k,i})$. We again introduce a *best pocket* iterate, denoted by $\boldsymbol{w}_{k,i}^{\rm best}$. At any iteration i, the value that is saved in the pocket variable is the iterate, $\boldsymbol{w}_{k,j}$, that has generated the smallest mean risk value up to time i, i.e.,

$$\boldsymbol{w}_{k,i}^{\rm best} \;\stackrel{\Delta}{=}\; \arg\min_{1\leq j\leq i} \mathbb{E}\; J_k(\boldsymbol{w}_{k,j}). \tag{131}$$

Observe that we now have N pocket values, one for each agent k.

Theorem 5 (Network performance**)** *Consider using the stochastic sub-gradient diffusion algorithm (126) to seek the unique minimizer, $w^\star$, of the optimization problem (124), where the risk functions, $J_k(w)$, are assumed to satisfy Assumptions 1–3 with parameters $\{\eta_k, \beta_k^2, \sigma_k^2, e_k^2, f_k^2\}$. Assume the step-size parameter is sufficiently small (see condition (188)). Then, it holds that*

$$\mathbb{E}\left(\sum_{k=1}^N p_k J_k(\boldsymbol{w}_{k,i}^{\rm best}) - \sum_{k=1}^N p_k J_k(w^\star)\right) \leq \xi\cdot\alpha_q^i \sum_{k=1}^N p_k \|w_{k,0}-w^\star\| + \frac{\mu}{2}\sum_{k=1}^N \left(p_k f_k^2 + p_k^2\sigma_k^2 + 2p_k f_k h\right) \tag{132}$$

for some finite constants h and ξ. The convergence to steady-state regime occurs at an exponential rate, $O(\alpha_q^i)$, dictated by the parameter

$$\alpha_q \;\stackrel{\Delta}{=}\; \max_k \left\{1-\mu\eta_k+\mu^2 e_k^2 + \mu^2\beta_k^2 p_k + \mu^2 h\frac{e_k^2}{f_k}\right\} = 1 - O(\mu). \tag{133}$$

Condition (188) further ahead ensures $\alpha \in (0,1)$.

Proof : The argument is provided in Appendix B. ■

The above theorem clarifies the performance of the network in terms of the best pocket values across the agents. However, these pocket values are not readily available because the risk values, $J_k(\boldsymbol{w}_{k,i})$, cannot be evaluated. This is due to the fact that the statistical properties of the data are not known beforehand. As was the case with the single-agent scenario, a more practical conclusion can be deduced from the statement of the theorem as follows. We again introduce the geometric sum

$$S_L \;\stackrel{\Delta}{=}\; \sum_{j=1}^L \alpha_q^{L-j} \;=\; \frac{1-\alpha_q^L}{1-\alpha_q}, \tag{134}$$

as well as the normalized and convex-combination coefficients:

$$r_L(j) \;\stackrel{\Delta}{=}\; \frac{\alpha_q^{L-j}}{S_L}, \quad j=1,2,\ldots,L. \tag{135}$$

Using these coefficients, we define a weighted iterate at each agent:

$$\bar{\boldsymbol{w}}_{k,L} \;\stackrel{\Delta}{=}\; \sum_{j=1}^L r_L(j)\boldsymbol{w}_{k,j} = \frac{1}{S_L}\left[\alpha_q^{L-1}\boldsymbol{w}_{k,1} + \ldots + \alpha_q \boldsymbol{w}_{k,L-1} + \boldsymbol{w}_{k,L}\right], \tag{136}$$

and observe that $\bar{\boldsymbol{w}}_{k,L}$ satisfies the recursive construction:

$$\bar{\boldsymbol{w}}_{k,L} \;=\; \left(1-\frac{1}{S_L}\right)\bar{\boldsymbol{w}}_{k,L-1} \;+\; \frac{1}{S_L}\boldsymbol{w}_{k,L}. \tag{137}$$

In particular, as $L\to\infty$, we have $S_L\to 1/(1-\alpha_q)$, and the above recursion simplifies in the limit to

$$\bar{\boldsymbol{w}}_{k,L} \;=\; \alpha_q\bar{\boldsymbol{w}}_{k,L-1} \;+\; (1-\alpha_q)\boldsymbol{w}_{k,L}. \tag{138}$$

Corollary 6 (Weighted iterates) *Under the same conditions as in Theorem 5, it holds that*

$$\lim_{L\to\infty}\;\mathbb{E}\left(\sum_{k=1}^{N}p_kJ_k(\bar{\boldsymbol{w}}_{k,L})-\sum_{k=1}^{N}p_kJ_k(w^\star)\right)\leq\frac{\mu}{2}\sum_{k=1}^{N}\Big(p_kf_k^2+p_k^2\sigma_k^2+2hp_kf_k\Big)\;=\;O(\mu) \tag{139}$$

and convergence continues to occur at the same exponential rate, $O(\alpha_q^L)$. ■

Result (139) is an interesting conclusion. However, the statement is in terms of the averaged iterate $\bar{\boldsymbol{w}}_{k,L}$ whose computation requires knowledge of α_q. This latter parameter is a global information, which is not readily available to all agents. Nevertheless, result (139) motivates the following useful distributed implementation with a similar guaranteed performance bound. We can replace α_q by a design parameter, κ, that is no less than α_q but still smaller than one, i.e., $\alpha_q\leq\kappa<1$. Next, we introduce the weighted variable:

$$\bar{\boldsymbol{w}}'_{k,L} \;\;\stackrel{\Delta}{=}\;\; \sum_{j=1}^{L}r'_L(j)\boldsymbol{w}_{k,j}, \tag{140}$$

where

$$r'_L(j)=\kappa^{L-j}/S'_L,\;\;\; j=1,2\ldots,L, \tag{141}$$

and

$$S'_L=\sum_{j=1}^{L}\kappa^{L-j}. \tag{142}$$

Corollary 7 (Distributed Weighted iterates) *Under the same conditions as in Theorem 5 and $\alpha_q\leq\kappa<1$, relation (139) continues to hold with $\bar{\boldsymbol{w}}_{k,L}$ replaced by $\bar{\boldsymbol{w}}'_{k,L}$. Moreover, convergence now occurs at the exponential rate $O(\kappa^L)$.* ■

6.4 Interpretation of Results

Examining the bound in (139), and comparing it with result (94) for the single-agent case, we observe that the topology of the network is now reflected in the bound through the Perron entries, p_k. Recall from (128) that the $\{p_k\}$ are the entries of the right-eigenvector of A corresponding to the eigenvalue at one. Moreover, the bound in (139)involves three terms (rather than only two as in the single-agent case):

(1) $p_k f_k^2$, which arises from the non-smoothness of the risk function;

(2) $p_k^2 \sigma_k^2$, which is due to gradient noise and the approximation of the true sub-gradient vector;

(3) $2hp_k f_k$, which is an extra term in comparison to the single agent case. We explained in (178) that the value of h is related to how far the error at each agent is away from the weighted average error across the network. Therefore, the term $2hp_k f_k$ is induced by the distributed cooperative strategy.

Additionally, when the risk function happens to be smooth, we have $f_k^2 = 0$. But we cannot set $R = f_k$ any more. Instead, we can set R to be a small number, say $\mu^{1/2}$. Relation (181) will then give:

$$\begin{aligned}\mathbb{E}\,\bar{g}(\boldsymbol{\mathcal{W}}_{i-1})^{\mathsf{T}}\bar{\boldsymbol{w}}_{i-1} \leq &\sum_{k=1}^{N} p_k\Big(J_k(w^\star) - \mathbb{E}\,J_k(\boldsymbol{w}_{k,i-1}) - \frac{\eta_k}{2}\mathbb{E}\,\|\widetilde{\boldsymbol{w}}_{k,i-1}\|^2\Big) \\ &+ \frac{h}{2}\sum_{k=1}^{N} p_k\big(\mu^{1/2}e_k^2\mathbb{E}\,\|\widetilde{\boldsymbol{w}}_{k,i-1}\|^2 + \mu^{3/2}\big). \end{aligned} \tag{143}$$

Hence, we can recover the tighter result:

$$\lim_{L\to\infty}\ \mathbb{E}\sum_{k=1}^{N} p_k J_k(\bar{\boldsymbol{w}}_{k,L}) - \sum_{k=1}^{N} p_k J_k(w^\star) \leq \frac{\mu}{2}\sum_{k=1}^{N} p_k^2\sigma_k^2 + o(\mu). \tag{144}$$

This bound is similar to the one derived in (Sayed, 2014a) except for a factor of two ($\mu/2$ instead of $\mu/4$) since the derivation in the current article does not require the cost functions to be twice-differentiable.

Example 8 (Multi-agent LASSO problem) We now consider the LASSO problem with 20 agents connected according to Fig. 6(left). Each agent has different regression power and noise level, as illustrated in Fig. 6(right). The remaining parameters, including $\boldsymbol{w}^\circ, \delta, \mu$ and M are the same as in Example 5. The parameter $h \approx 1.8$ is computed from the simulation directly. Figure. 7 compares several strategies including standard diffusion LMS(Cattivelli and Sayed, 2010; Sayed, 2014a,b)

$$\begin{cases} \boldsymbol{\psi}_{k,i} = \boldsymbol{w}_{k,i-1} + \mu\boldsymbol{h}_{k,i}(\boldsymbol{\gamma}(k,i) - \boldsymbol{h}_{k,i}^{\mathsf{T}}\boldsymbol{w}_{k,i-1}) \\ \boldsymbol{w}_{k,i} = \sum_{\ell\in\mathcal{N}_k} a_{\ell k}\boldsymbol{\psi}_{\ell,i} \end{cases}, \tag{145}$$

and sparse diffusion LMS(Di Lorenzo et al., 2012; Di Lorenzo and Sayed, 2013; Liu et al., 2012; Chouvardas et al., 2012):

$$\begin{cases} \boldsymbol{\psi}_{k,i} = \boldsymbol{w}_{k,i-1} + \mu\boldsymbol{h}_{k,i}(\boldsymbol{\gamma}(k,i) - \boldsymbol{h}_{k,i}^{\mathsf{T}}\boldsymbol{w}_{k,i-1}) - \mu\delta\cdot\mathrm{sgn}(\boldsymbol{w}_{k,i-1}) \\ \boldsymbol{w}_{k,i} = \sum_{\ell\in\mathcal{N}_k} a_{\ell k}\boldsymbol{\psi}_{\ell,i} \end{cases}, \tag{146}$$

in the cooperative and non-cooperative modes of operation (in the latter case, the combination step (126) is absent).

□

Example 9 (Multi-agent SVM learning) We examine the diffusion sub-gradient SVM implementation:

$$\begin{cases} \boldsymbol{\psi}_{k,i} = (1-\rho\mu)\boldsymbol{w}_{k,i-1} - \mu\boldsymbol{\gamma}(k,i)\boldsymbol{h}_i\mathbb{I}[\boldsymbol{\gamma}(k,i)\boldsymbol{h}_{k,i}^{\mathsf{T}}\boldsymbol{w}_{k,i-1} \leq 1] \\ \boldsymbol{w}_{k,i} = \displaystyle\sum_{\ell\in\mathcal{N}_k} a_{\ell k}\boldsymbol{\psi}_{\ell,i} \\ S_{k,i} = \kappa S_{k,i-1} + 1 \\ \bar{\boldsymbol{w}}_{k,i} = \left(1 - \dfrac{1}{S_{k,i}}\right)\bar{\boldsymbol{w}}_{k,i-1} + \dfrac{1}{S_{k,i}}\boldsymbol{w}_{k,i} \end{cases}, \tag{147}$$

(with all variables initiated at zero) over the Adult dataset again. We distribute 32561 training data over a network consisting of 20 agents. We set $\rho = 0.002$ and $\mu = 0.15$ for all agents. From Example 6 and Theorem 5, we know that for the multi-agent SVM problem:

$$\begin{aligned} \alpha_q &= \max_k \left\{1 - \mu\rho + \mu^2(h+1)e_k^2\right\} \\ &= \max_k \left\{1 - \mu\rho + \mu^2(h+1)\left(\rho^2 + \frac{2\rho d_k}{R}\right)\right\}. \end{aligned} \tag{148}$$

We set $\kappa = 1 - 0.9\cdot\mu\rho$, which usually guarantees $\kappa \geq \alpha_q$. Fig. 8 (left) shows that cooperation among the agents outperforms the non-cooperative solution. Moreover, the distributed network can almost match the performance of the centralized LIBSVM solution. We also examined the RCV1 dataset. Here we have 20242 training data points and we distribute them over 20 agents. We set the parameters to $\rho = 1\times 10^{-5}$ and $\mu = 0.5$(for limited data). We now use $\kappa = 1 - 0.5\cdot\mu\rho$ since μ is not that small. The result is shown in Fig. 8 (right).

□

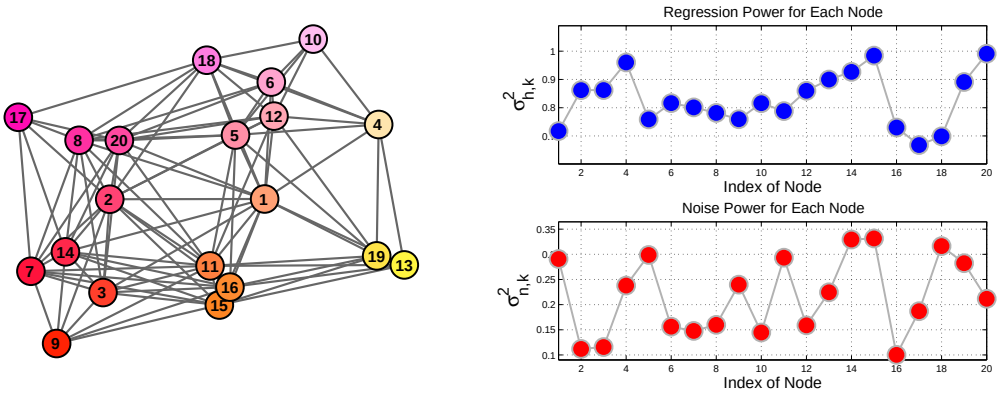

Figure 6: Left: Network topology linking $N = 20$ agents. Right: Feature and noise variances across the agents.

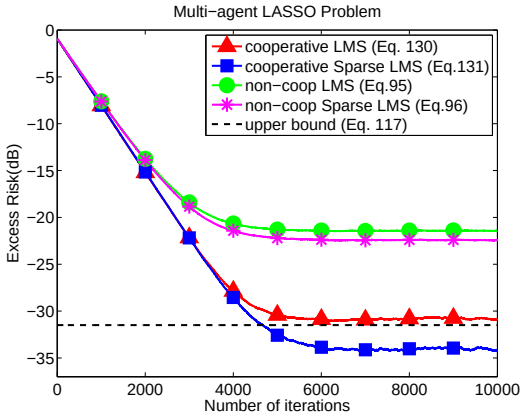

Figure 7: The excess-risk curves(Eq. 117) for several strategies.

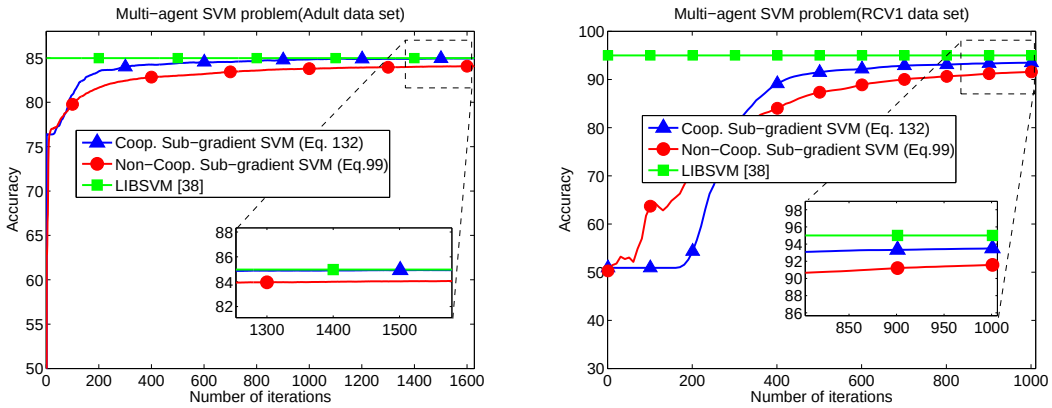

Figure 8: Performance of multi-agent SVM solution for the Adult dataset(Left) and RCV1 dataset(Right), where vertical axis measures the percentage of correct prediction over test dataset.

7. Conclusion

In summary, we examined the performance of stochastic sub-gradient learning strategies. We proposed a new affine-Lipschitz condition, which is quite suitable for strongly convex but non-differentiable cost functions and is applicable to several important cases including SVM, LASSO, Total-Variation denoising, etc. Under this weaker condition, the analysis establishes that sub-gradient strategies can attain exponential convergence rates, as opposed to sub-linear rates. The analysis also established that these strategies can approach the optimal solution within $O(\mu)$, for sufficiently small step-size. Both single-agent and multi-agent scenarios are studied.

Acknowledgments

This work was supported in part by NSF grants CIF-1524250, ECCS-1407712 and DARPA N66001-14-2-4029. The authors would like to thank PhD student Kun Yuan for valuable feedback on the multi-agent case.

Appendix A. Derivation of the Tighter SVM Bound (114)

We assumed in the exposition leading to Theorem 1 and Corollary 2 that the sub-gradient vectors and the variance of the gradient noise satisfy affine-like forms separately — see (24) and (28). For the case of the SVM problem, a joint bound can be derived as follows. First, note that

$$\begin{aligned}
&\mathbb{E}\,\Big[\,\|g^{\rm svm}(\boldsymbol{w}_{i-1})+\boldsymbol{s}_i(\boldsymbol{w}_{i-1})\|^2\,|\,\boldsymbol{\mathcal{F}}_{i-1}\Big] \\
&\qquad=\mathbb{E}\,\Big[\,\|\widehat{g}^{\rm svm}(\boldsymbol{w}_{i-1})\|^2\,|\,\boldsymbol{\mathcal{F}}_{i-1}\Big] \\
&\qquad=\mathbb{E}\,\Big[\,\Big\|\rho\boldsymbol{w}_{i-1}+\boldsymbol{\gamma}(i)\boldsymbol{h}_i\,\mathbb{I}[\boldsymbol{\gamma}(i)\boldsymbol{h}_i^{\mathsf{T}}\boldsymbol{w}_{i-1}\le 1]\Big\|^2\,|\,\boldsymbol{\mathcal{F}}_{i-1}\Big] \\
&\qquad=\rho^2\|\boldsymbol{w}_{i-1}\|^2+2\rho\mathbb{E}\,\boldsymbol{\gamma}(i)\boldsymbol{h}_i^{\mathsf{T}}\boldsymbol{w}_{i-1}\,\mathbb{I}[\boldsymbol{\gamma}(i)\boldsymbol{h}_i^{\mathsf{T}}\boldsymbol{w}_{i-1}\le 1]\,|\,\boldsymbol{\mathcal{F}}_{i-1}]+ \\
&\qquad\quad\mathbb{E}\,\Big[\boldsymbol{\gamma}^2(i)\boldsymbol{h}_i\boldsymbol{h}_i^{\mathsf{T}}\,\mathbb{I}[\boldsymbol{\gamma}(i)\boldsymbol{h}_i^{\mathsf{T}}\boldsymbol{w}_{i-1}\le 1]\,|\,\boldsymbol{\mathcal{F}}_{i-1}\Big] \\
&\qquad\overset{(a)}{\le}\rho^2\|\boldsymbol{w}_{i-1}\|^2+2\rho+\mathbb{E}\,[\boldsymbol{h}_i^{\mathsf{T}}\boldsymbol{h}_i\,\mathbb{I}[\boldsymbol{\gamma}(i)\boldsymbol{h}_i^{\mathsf{T}}\boldsymbol{w}_{i-1}\le 1]\,|\,\boldsymbol{\mathcal{F}}_{i-1}] \\
&\qquad\le\rho^2\|\boldsymbol{w}_{i-1}\|^2+2\rho+{\rm Tr}(R_h) \\
&\qquad\overset{(b)}{\le}2\rho^2\|\widetilde{\boldsymbol{w}}_{i-1}\|^2+2\rho^2\|w^\star\|^2+2\rho+{\rm Tr}(R_h),
\end{aligned}\tag{149}$$

where in step (a) we used the facts that $\boldsymbol{\gamma}^2(i)=1$ and

$$\boldsymbol{\gamma}(i)\boldsymbol{h}_i^{\mathsf{T}}\boldsymbol{w}_{i-1}\mathbb{I}[\boldsymbol{\gamma}(i)\boldsymbol{h}_i^{\mathsf{T}}\boldsymbol{w}_{i-1}\le 1]\,|\,\boldsymbol{\mathcal{F}}_{i-1}]\le 1,\tag{150}$$

while step (b) follows from Jensen's inequality by adding and subtracting $w^\star$ to $\boldsymbol{w}_{i-1}$. We therefore conclude that

$$\mathbb{E}\,[\|g^{\rm svm}(\boldsymbol{w}_{i-1})+\boldsymbol{s}_i(\boldsymbol{w}_{i-1})\|^2\,|\,\boldsymbol{\mathcal{F}}_{i-1}]\le 2\rho^2\|\widetilde{\boldsymbol{w}}_{i-1}\|^2+2\rho^2\|w^\star\|^2+2\rho+{\rm Tr}(R_h).\tag{151}$$

We now use this result to expand the first line of (64).

$$\begin{aligned}
\mathbb{E}\,[\|\widetilde{\boldsymbol{w}}_i\|^2\,|\,\boldsymbol{\mathcal{F}}_{i-1}\,] &= \mathbb{E}\,[\,\|\widetilde{\boldsymbol{w}}_{i-1}+\mu g^{\rm svm}(\boldsymbol{w}_{i-1})+\mu\boldsymbol{s}_i(\boldsymbol{w}_{i-1})\|^2\,|\,\boldsymbol{\mathcal{F}}_{i-1}\,] \\
&= \|\widetilde{\boldsymbol{w}}_{i-1}\|^2+2\mu g(\boldsymbol{w}_{i-1})^{\mathsf{T}}\widetilde{\boldsymbol{w}}_{i-1}+\mu^2\mathbb{E}\,[\|g^{\rm svm}(\boldsymbol{w}_{i-1})+\boldsymbol{s}_i(\boldsymbol{w}_{i-1})\|^2\,|\,\boldsymbol{\mathcal{F}}_{i-1}\,] \\
&\le \|\widetilde{\boldsymbol{w}}_{i-1}\|^2+2\mu g(\boldsymbol{w}_{i-1})^{\mathsf{T}}\widetilde{\boldsymbol{w}}_{i-1}+\mu^2\big(2\rho^2\|\widetilde{\boldsymbol{w}}_{i-1}\|^2+2\rho^2\|w^\star\|^2+2\rho+{\rm Tr}(R_h)\big).
\end{aligned}\tag{152}$$

Now following the same steps after (65) , we arrive at the tighter bound (114).

Appendix B. Proof of theorem 5

Introduce the error vector, $\widetilde{\boldsymbol{w}}_{k,i} = w^\star - w_{k,i}$. We collect the iterates and the respective errors from across the network into block column vectors:

$$\boldsymbol{\mathcal{W}}_i \triangleq \mathrm{col}\{\boldsymbol{w}_{1,i}, \boldsymbol{w}_{2,i}, \ldots, \boldsymbol{w}_{N,i}\} \tag{153}$$

$$\widetilde{\boldsymbol{\mathcal{W}}}_i \triangleq \mathrm{col}\{\widetilde{\boldsymbol{w}}_{1,i}, \widetilde{\boldsymbol{w}}_{2,i}, \ldots, \widetilde{\boldsymbol{w}}_{N,i}\}. \tag{154}$$

We also define the extended quantities:

$$\mathcal{A} \triangleq A \otimes I_M \tag{155}$$

$$\boldsymbol{\mathcal{G}}(\boldsymbol{\mathcal{W}}_{i-1}) \triangleq \mathrm{col}\{g_1(\boldsymbol{w}_{1,i-1}), , \ldots, g_N(\boldsymbol{w}_{N,i-1})\} \tag{156}$$

$$\boldsymbol{\mathcal{s}}_i(\boldsymbol{\mathcal{W}}_{i-1}) \triangleq \mathrm{col}\{s_{1,i}(\boldsymbol{w}_{1,i-1}), \ldots, s_{N,i}(\boldsymbol{w}_{N,i-1})\}, \tag{157}$$

where $\otimes$ denotes the Kronecker product operation, and $\boldsymbol{s}_{k,i}(\boldsymbol{w}_{k,i-1})$ denotes the gradient noise at agent k. Then, it is straightforward to verify that the network error vector generated by the diffusion strategy evolves according to the following dynamics:

$$\widetilde{\boldsymbol{\mathcal{W}}}_i = \mathcal{A}^{\mathsf{T}} \left(\widetilde{\boldsymbol{\mathcal{W}}}_{i-1} + \mu \boldsymbol{\mathcal{G}}(\boldsymbol{\mathcal{W}}_{i-1}) + \mu \boldsymbol{\mathcal{s}}_i(\boldsymbol{\mathcal{W}}_{i-1})\right). \tag{158}$$

Motivated by the treatment of the smooth case in (Sayed, 2014a; Chen and Sayed, 2015a,b), we perform a useful change of variables. Let $\mathcal{V}_\epsilon = V_\epsilon \otimes I_M$ and $\mathcal{J}_\epsilon = J_\epsilon \otimes I_M$. Multiplying (158) from the left by $\mathcal{V}_\epsilon^{\mathsf{T}}$ gives

$$\mathcal{V}_\epsilon^{\mathsf{T}} \widetilde{\boldsymbol{\mathcal{W}}}_i = \mathcal{J}_\epsilon^{\mathsf{T}} \left[\mathcal{V}_\epsilon^{\mathsf{T}} \widetilde{\boldsymbol{\mathcal{W}}}_{i-1} + \mu \mathcal{V}_\epsilon^{\mathsf{T}} \boldsymbol{\mathcal{G}}(\boldsymbol{\mathcal{W}}_{i-1}) + \mu \mathcal{V}_\epsilon^{\mathsf{T}} \boldsymbol{\mathcal{s}}_i(\boldsymbol{\mathcal{W}}_{i-1})\right]. \tag{159}$$

We introduce the transformed quantities:

$$\mathcal{V}_\epsilon^{\mathsf{T}} \widetilde{\boldsymbol{\mathcal{W}}}_i = \begin{bmatrix} (p^{\mathsf{T}} \otimes I)\widetilde{\boldsymbol{\mathcal{W}}}_i \\ (V_R^{\mathsf{T}} \otimes I)\widetilde{\boldsymbol{\mathcal{W}}}_i \end{bmatrix} \triangleq \begin{bmatrix} \bar{\boldsymbol{w}}_i \\ \check{\boldsymbol{\mathcal{W}}}_i \end{bmatrix}, \tag{160}$$

$$\mathcal{V}_\epsilon^{\mathsf{T}} \boldsymbol{\mathcal{G}}(\boldsymbol{\mathcal{W}}_{i-1}) = \begin{bmatrix} (p^{\mathsf{T}} \otimes I)\boldsymbol{\mathcal{G}}(\boldsymbol{\mathcal{W}}_{i-1}) \\ (V_R^{\mathsf{T}} \otimes I)\boldsymbol{\mathcal{G}}(\boldsymbol{\mathcal{W}}_{i-1}) \end{bmatrix} \triangleq \begin{bmatrix} \bar{g}(\boldsymbol{\mathcal{W}}_{i-1}) \\ \check{\boldsymbol{\mathcal{G}}}(\boldsymbol{\mathcal{W}}_{i-1}) \end{bmatrix}, \tag{161}$$

$$\mathcal{V}_\epsilon^{\mathsf{T}} \boldsymbol{\mathcal{s}}_i(\boldsymbol{\mathcal{W}}_{i-1}) = \begin{bmatrix} (p^{\mathsf{T}} \otimes I)\boldsymbol{\mathcal{s}}_i(\boldsymbol{\mathcal{W}}_{i-1}) \\ (V_R^{\mathsf{T}} \otimes I)\boldsymbol{\mathcal{s}}_i(\boldsymbol{\mathcal{W}}_{i-1}) \end{bmatrix} \triangleq \begin{bmatrix} \bar{\boldsymbol{s}}_i(\boldsymbol{\mathcal{W}}_{i-1}) \\ \check{\boldsymbol{s}}_i(\boldsymbol{\mathcal{W}}_{i-1}) \end{bmatrix}. \tag{162}$$

Note that the quantities $\{\bar{\boldsymbol{w}}_i, \bar{g}(\boldsymbol{\mathcal{W}}_{i-1}), \bar{\boldsymbol{s}}_i(\boldsymbol{\mathcal{W}}_{i-1})\}$ amount to the weighted averages:

$$\bar{\boldsymbol{w}}_i = \sum_{k=1}^N p_k \widetilde{\boldsymbol{w}}_{k,i}, \tag{163}$$

$$\bar{g}(\boldsymbol{\mathcal{W}}_{i-1}) = \sum_{k=1}^N p_k g_k(\boldsymbol{w}_{k,i-1}), \tag{164}$$

$$\bar{\boldsymbol{s}}_i(\boldsymbol{\mathcal{W}}_{i-1}) = \sum_{k=1}^N p_k \boldsymbol{s}_{k,i}(\boldsymbol{w}_{k,i-1}). \tag{165}$$

We can now rewrite (159) as

$$\left[\begin{array}{c} \bar{\boldsymbol{w}}_i \\ \check{\boldsymbol{\mathcal{W}}}_i \end{array}\right] = \left[\begin{array}{c|c} I_M & 0 \\ \hline 0 & \mathcal{J}_\epsilon^{\mathsf{T}} \end{array}\right] \left(\left[\begin{array}{c} \bar{\boldsymbol{w}}_{i-1} \\ \check{\boldsymbol{\mathcal{W}}}_{i-1} \end{array}\right] + \mu \left[\begin{array}{c} \bar{g}(\boldsymbol{\mathcal{W}}_{i-1}) \\ \check{\boldsymbol{\mathcal{G}}}(\boldsymbol{\mathcal{W}}_{i-1}) \end{array}\right] + \mu \left[\begin{array}{c} \bar{\boldsymbol{s}}_i(\boldsymbol{\mathcal{W}}_{i-1}) \\ \check{\boldsymbol{s}}_i(\boldsymbol{\mathcal{W}}_{i-1}) \end{array}\right] \right). \tag{166}$$

Consider the top recursion, namely,

$$\bar{\boldsymbol{w}}_i = \bar{\boldsymbol{w}}_{i-1} + \mu \bar{g}(\boldsymbol{\mathcal{W}}_{i-1}) + \mu \bar{\boldsymbol{s}}_i(\boldsymbol{\mathcal{W}}_{i-1}). \tag{167}$$

Squaring and taking expectations we have

$$\begin{aligned} \mathbb{E}\,[\|\bar{\boldsymbol{w}}_i\|^2 \,|\, \boldsymbol{\mathcal{F}}_{i-1}] &= \mathbb{E}\,[\|\bar{\boldsymbol{w}}_{i-1} + \mu \bar{g}(\boldsymbol{\mathcal{W}}_{i-1}) + \mu \bar{\boldsymbol{s}}_i(\boldsymbol{\mathcal{W}}_{i-1})\|^2 \,|\, \boldsymbol{\mathcal{F}}_{i-1}] \\ &= \|\bar{\boldsymbol{w}}_{i-1}\|^2 + 2\mu \bar{g}(\boldsymbol{\mathcal{W}}_{i-1})^{\mathsf{T}} \bar{\boldsymbol{w}}_{i-1} \;+ \mu^2 \|\bar{g}(\boldsymbol{\mathcal{W}}_{i-1})\|^2 \;+\; \mu^2 \mathbb{E}\,[\|\bar{\boldsymbol{s}}_i(\boldsymbol{\mathcal{W}}_{i-1})\|^2 \,|\, \boldsymbol{\mathcal{F}}_{i-1}]. \end{aligned} \tag{168}$$

We examine the terms on the right-hand side one by one. First note that, using Jensen's inequality,

$$\begin{aligned} \|\bar{g}(\boldsymbol{\mathcal{W}}_{i-1})\|^2 &= \left\| \sum_{k=1}^N p_k g_k(\boldsymbol{w}_{k,i-1}) \right\|^2 \\ &\leq \sum_{k=1}^N p_k \|g_k(\boldsymbol{w}_{k,i-1})\|^2 \\ &\overset{(a)}{=} \sum_{k=1}^N p_k \|g_k(\boldsymbol{w}_{k,i-1}) - g_k'(w^\star)\|^2 \\ &\overset{(50)}{\leq} \sum_{k=1}^N p_k \Big(e_k^2 \|\widetilde{\boldsymbol{w}}_{k,i-1}\|^2 + f_k^2 \Big). \end{aligned} \tag{169}$$

In step (a), we exploit the assumption that the individual risks share a common minimizer, $w^\star$, which implies that there exists one particular sub-gradient $g_k'(w^\star)$ for each agent k, satisfying $g_k'(w^\star) = 0$.

Next, using the assumed independence of the stochastic gradient noises across the agents, we have

$$\begin{aligned} \mathbb{E}\,[\|\bar{\boldsymbol{s}}_i(\boldsymbol{\mathcal{W}}_{i-1})\|^2 \,|\, \boldsymbol{\mathcal{F}}_{i-1}] &= \mathbb{E}\,\left[\left\| \sum_{k=1}^N p_k \boldsymbol{s}_k(\boldsymbol{w}_{k,i-1}) \right\|^2 \,|\, \boldsymbol{\mathcal{F}}_{i-1} \right] \\ &= \sum_{k=1}^N p_k^2 \mathbb{E}\,[\|\boldsymbol{s}_k(\boldsymbol{w}_{k,i-1})\|^2 \,|\, \boldsymbol{\mathcal{F}}_{i-1}] \\ &\leq \sum_{k=1}^N p_k^2 \Big(\beta_k^2 \|\widetilde{\boldsymbol{w}}_{k,i-1}\|^2 + \sigma_k^2 \Big). \end{aligned} \tag{170}$$

Finally, with regards to the cross term in (168), we adapt an argument from (Nedic and Ozdaglar, 2009) to note that:

$$\bar{g}(\boldsymbol{\mathcal{W}}_{i-1})^{\mathsf{T}} \bar{\boldsymbol{w}}_{i-1} = \sum_{k=1}^N p_k g_k^{\mathsf{T}}(\boldsymbol{w}_{k,i-1}) \big(\widetilde{\boldsymbol{w}}_{k,i-1} + \bar{\boldsymbol{w}}_{i-1} - \widetilde{\boldsymbol{w}}_{k,i-1} \big)$$

$$= \sum_{k=1}^{N} p_k g_k^{\mathsf{T}}(\boldsymbol{w}_{k,i-1})\widetilde{\boldsymbol{w}}_{k,i-1} + \sum_{k=1}^{N} p_k g_k^{\mathsf{T}}(\boldsymbol{w}_{k,i-1})\big(\bar{\boldsymbol{w}}_{i-1} - \widetilde{\boldsymbol{w}}_{k,i-1}\big). \tag{171}$$

Using the strong-convexity property, namely,

$$g_k(\boldsymbol{w}_{k,i-1})^{\mathsf{T}}\widetilde{\boldsymbol{w}}_{k,i-1} \leq J_k(w^\star) - J_k(\boldsymbol{w}_{k,i-1}) - \frac{\eta_k}{2}\|\widetilde{\boldsymbol{w}}_{k,i-1}\|^2, \tag{172}$$

we get

$$\begin{aligned}
\bar{g}(\boldsymbol{\mathcal{W}}_{i-1})^{\mathsf{T}}\bar{\boldsymbol{w}}_{i-1} &\leq \sum_{k=1}^{N} p_k\Big(J_k(w^\star) - J_k(\boldsymbol{w}_{k,i-1}) - \frac{\eta_k}{2}\|\widetilde{\boldsymbol{w}}_{k,i-1}\|^2\Big) + \\
&\quad \sum_{k=1}^{N} p_k g_k^{\mathsf{T}}(\boldsymbol{w}_{k,i-1})\big(\bar{\boldsymbol{w}}_{i-1} - \widetilde{\boldsymbol{w}}_{k,i-1}\big) \qquad (173)\\
&\leq \sum_{k=1}^{N} p_k\Big(J_k(w^\star) - J_k(\boldsymbol{w}_{k,i-1}) - \frac{\eta_k}{2}\|\widetilde{\boldsymbol{w}}_{k,i-1}\|^2\Big) + \\
&\quad \sum_{k=1}^{N} p_k\|g_k(\boldsymbol{w}_{k,i-1})\|\|\bar{\boldsymbol{w}}_{i-1} - \widetilde{\boldsymbol{w}}_{k,i-1}\|. \qquad (174)
\end{aligned}$$

It follows, under expectation, that

$$\begin{aligned}
\mathbb{E}\,\bar{g}(\boldsymbol{\mathcal{W}}_{i-1})^{\mathsf{T}}\bar{\boldsymbol{w}}_{i-1} &\leq \sum_{k=1}^{N} p_k\Big(J_k(w^\star) - \mathbb{E}\,J_k(\boldsymbol{w}_{k,i-1}) - \frac{\eta_k}{2}\mathbb{E}\,\|\widetilde{\boldsymbol{w}}_{k,i-1}\|^2\Big) + \\
&\quad \sum_{k=1}^{N} p_k\mathbb{E}\,\left(\|g_k(\boldsymbol{w}_{k,i-1})\|\|\bar{\boldsymbol{w}}_{i-1} - \widetilde{\boldsymbol{w}}_{k,i-1}\|\right). \qquad (175)
\end{aligned}$$

Now, using the Cauchy-Schwartz inequality, we can bound the last expectation as

$$\mathbb{E}\left(\|g_k(\boldsymbol{w}_{k,i-1})\|\|\bar{\boldsymbol{w}}_{i-1} - \widetilde{\boldsymbol{w}}_{k,i-1}\|\right) \leq \sqrt{\mathbb{E}\,\|g_k(\boldsymbol{w}_{k,i-1})\|^2\mathbb{E}\,\|\bar{\boldsymbol{w}}_{i-1} - \widetilde{\boldsymbol{w}}_{k,i-1}\|^2}. \tag{176}$$

After sufficient iterations, it will hold that (see Appendix C for the proof):

$$\mathbb{E}\,\|\bar{\boldsymbol{w}}_{i-1} - \widetilde{\boldsymbol{w}}_{k,i-1}\|^2 = O(\mu^2). \tag{177}$$

This means that there exists an I_o large enough and a constant h such that for all $i \geq I_o$:

$$\mathbb{E}\,\|\bar{\boldsymbol{w}}_{i-1} - \widetilde{\boldsymbol{w}}_{k,i-1}\|^2 \leq h^2\mu^2. \tag{178}$$

Therefore, we find that

$$\begin{aligned}
\mathbb{E}\left(\|g_k(\boldsymbol{w}_{k,i-1})\|\|\bar{\boldsymbol{w}}_{i-1} - \widetilde{\boldsymbol{w}}_{k,i-1}\|\right) &\leq h\mu\,\left(\sqrt{\mathbb{E}\,\|g_k(\boldsymbol{w}_{k,i-1})\|^2}\right) \\
&\leq h\mu\,\left(\sqrt{e_k^2\mathbb{E}\,\|\widetilde{\boldsymbol{w}}_{k,i-1}\|^2 + f_k^2}\right)
\end{aligned}$$

$$\leq \mu\frac{h}{2}\left(\frac{e_k^2\mathbb{E}\,\|\widetilde{\boldsymbol{w}}_{k,i-1}\|^2+f_k^2}{R}+R\right), \tag{179}$$

where the last inequality follows from using

$$\sqrt{x}\leq\frac{1}{2}\Big(\frac{x}{R}+R\Big),\;\; x\geq 0, \tag{180}$$

for any positive R, e.g., $R=f_k$, which allows us to conclude that, as $i\to\infty$:

$$\begin{aligned}\mathbb{E}\,\bar{g}(\boldsymbol{\mathcal{W}}_{i-1})^{\mathsf{T}}\bar{\boldsymbol{w}}_{i-1}\leq&\sum_{k=1}^{N}p_k\Big(J_k(w^\star)-\mathbb{E}\,J_k(\boldsymbol{w}_{k,i-1})-\frac{\eta_k}{2}\mathbb{E}\,\|\widetilde{\boldsymbol{w}}_{k,i-1}\|^2\Big)\\&+\mu\frac{h}{2}\sum_{k=1}^{N}p_k\left(\frac{e_k^2}{f_k}\mathbb{E}\,\|\widetilde{\boldsymbol{w}}_{k,i-1}\|^2+2f_k\right).\end{aligned} \tag{181}$$

Taking expectation of (168) over the filtration and substituting (169), (170), and (181), we obtain asymptotically that:

$$\begin{aligned}\mathbb{E}\,\|\bar{\boldsymbol{w}}_i\|^2\;\;&\leq\;\;\mathbb{E}\,\|\bar{\boldsymbol{w}}_{i-1}\|^2+2\mu\sum_{k=1}^{N}p_k\Big(J_k(w^\star)-\mathbb{E}\,J_k(\boldsymbol{w}_{k,i-1})\Big)-\mu\sum_{k=1}^{N}p_k\eta_k\mathbb{E}\,\|\widetilde{\boldsymbol{w}}_{k,i-1}\|^2+\\&\quad\mu^2\sum_{k=1}^{N}p_k\Big(e_k^2\mathbb{E}\,\|\widetilde{\boldsymbol{w}}_{k,i-1}\|^2+f_k^2\Big)+\mu^2\sum_{k=1}^{N}p_k^2\Big(\beta_k^2\mathbb{E}\,\|\widetilde{\boldsymbol{w}}_{k,i-1}\|^2+\sigma_k^2\Big)+\\&\quad\mu^2h\sum_{k=1}^{N}p_k\Big(\frac{e_k^2}{f_k}\mathbb{E}\,\|\boldsymbol{w}_{k,i-1}\|^2+2f_k\Big)\\&\leq\;\;\mathbb{E}\,\|\bar{\boldsymbol{w}}_{i-1}\|^2+2\mu\sum_{k=1}^{N}p_k\Big(J_k(w^\star)-\mathbb{E}\,J_k(\boldsymbol{w}_{k,i-1})\Big)-\\&\quad\sum_{k=1}^{N}(1-\alpha_k)\,p_k\mathbb{E}\,\|\widetilde{\boldsymbol{w}}_{k,i-1}\|^2+\mu^2\sum_{k=1}^{N}\Big(p_kf_k^2+p_k^2\sigma_k^2+2hp_kf_k\Big),\end{aligned} \tag{182}$$

where we defined α_k in the second inequality as follows:

$$1-\alpha_k\;\stackrel{\Delta}{=}\;\mu\eta_k-\mu^2e_k^2-\mu^2p_k\beta_k^2-\mu^2h\frac{e_k^2}{f_k}. \tag{183}$$

Let q denote the index of the agent that has the smallest $1-\alpha_k$:

$$q\;=\;\arg\min_{1\leq k\leq N}\{1-\alpha_k\}. \tag{184}$$

Then, it holds that

$$\begin{aligned}\sum_{k=1}^{N}(1-\alpha_k)\,p_k\mathbb{E}\,\|\widetilde{\boldsymbol{w}}_{k,i-1}\|^2&\geq(1-\alpha_q)\sum_{k=1}^{N}p_k\mathbb{E}\,\|\widetilde{\boldsymbol{w}}_{k,i-1}\|^2\\&\geq(1-\alpha_q)\mathbb{E}\,\|\bar{\boldsymbol{w}}_{i-1}\|^2,\end{aligned} \tag{185}$$

where we used Jensen's inequality to deduce that

$$\|\bar{\boldsymbol{w}}_{i-1}\|^2 = \left\|\sum_{k=1}^{N} p_k \widetilde{\boldsymbol{w}}_{k,i-1}\right\|^2 \leq \sum_{k=1}^{N} p_k \|\widetilde{\boldsymbol{w}}_{k,i-1}\|^2. \tag{186}$$

It follows from (182) that

$$2\mu\Big(\sum_{k=1}^{N} p_k \left(\mathbb{E}\, J_k(\boldsymbol{w}_{k,i-1}) - J_k(w^\star)\right)\Big) \leq \alpha_q \mathbb{E}\,\|\bar{\boldsymbol{w}}_{i-1}\|^2 - \mathbb{E}\,\|\bar{\boldsymbol{w}}_i\|^2 + \mu^2 \sum_{k=1}^{N} (p_k f_k^2 + p_k^2 \sigma_k^2 + 2h p_k f_k). \tag{187}$$

This inequality recursion has a form similar to the one we encountered in (69) in the single agent case. The argument can now be continued similarly to arrive at the conclusions in the statement of the theorem and that stability is ensured for sufficiently small step-sizes satisfying

$$\mu < \frac{\eta_q}{e_q^2 + p_q \beta_q^2 + h e_q^2/f_q}. \tag{188}$$

This bound ensures that $\alpha_q \in (0,1)$.

Appendix C. Proof of (177)

We now establish the asymptotic result (177). Let

$$\bar{\boldsymbol{\mathcal{W}}}_i = \mathrm{col}\{\bar{\boldsymbol{w}}_i, \ldots, \bar{\boldsymbol{w}}_i\}, \tag{189}$$

where the vector $\bar{\boldsymbol{w}}_i$ is stacked N times to match the dimension of $\widetilde{\boldsymbol{\mathcal{W}}}_i$. We start from the second relation in the error recursion (166):

$$\check{\boldsymbol{\mathcal{W}}}_i = \mathcal{J}_\epsilon^{\mathsf{T}}\Big(\check{\boldsymbol{\mathcal{W}}}_{i-1} + \mu\check{\boldsymbol{\mathcal{G}}}(\boldsymbol{\mathcal{W}}_{i-1}) + \mu\check{\boldsymbol{s}}_i(\boldsymbol{\mathcal{W}}_{i-1})\Big), \tag{190}$$

and first explain how to recover $\widetilde{\boldsymbol{\mathcal{W}}}_i - \bar{\boldsymbol{\mathcal{W}}}_i$ from $\check{\boldsymbol{\mathcal{W}}}_i$. Consider the linear system of equations $\check{\boldsymbol{\mathcal{W}}}_i = \mathcal{V}_R^{\mathsf{T}}\widetilde{\boldsymbol{\mathcal{W}}}_i$, with coefficient matrix $\mathcal{V}_R^{\mathsf{T}}$. Noting from (130) that $V_L^{\mathsf{T}} V_R = I$, we conclude from the relationship between the nullspace and range space of a matrix that (Laub, 2005):

$$\widetilde{\boldsymbol{\mathcal{W}}}_i - \mathcal{V}_L\check{\boldsymbol{\mathcal{W}}}_i \in \mathcal{N}(\mathcal{V}_R^{\mathsf{T}}) \iff \widetilde{\boldsymbol{\mathcal{W}}}_i = \mathcal{V}_L\check{\boldsymbol{\mathcal{W}}}_i + \boldsymbol{\mathcal{Z}}, \tag{191}$$

for some $\boldsymbol{\mathcal{Z}} \in \mathcal{N}(\mathcal{V}_R^{\mathsf{T}})$. We further know that $\mathcal{N}(V_R^{\mathsf{T}})$ is the linear space generated by the vector $\mathbb{1}$, so that $\boldsymbol{\mathcal{Z}}$ is parallel to the vector $\mathbb{1}$. Therefore, we can write $\boldsymbol{\mathcal{Z}} = \mathbb{1} \otimes z$, for some vector z. Moreover, it holds that

$$\begin{aligned}
\bar{\boldsymbol{w}}_i &= (p^{\mathsf{T}} \otimes I)\widetilde{\boldsymbol{\mathcal{W}}}_i \\
&= (p^{\mathsf{T}} \otimes I)\mathcal{V}_L\check{\boldsymbol{\mathcal{W}}}_i + (p^{\mathsf{T}} \otimes I)\boldsymbol{\mathcal{Z}} \\
&\overset{(a)}{=} (p^{\mathsf{T}} \otimes I)(\mathbb{1} \otimes z) \\
&\overset{(b)}{=} z,
\end{aligned} \tag{192}$$

where step (a) is because $(p^{\mathsf{T}} \otimes I)\mathcal{V}_L = (p^{\mathsf{T}} V_L) \otimes I = 0$, and step (b) is because of (129). Hence, combining the above two results, we find that

$$\widetilde{\boldsymbol{\mathcal{W}}}_i - \bar{\boldsymbol{\mathcal{W}}}_i = \mathcal{V}_L \check{\boldsymbol{\mathcal{W}}}_i, \tag{193}$$

which shows how we can recover $\widetilde{\boldsymbol{\mathcal{W}}}_i - \bar{\boldsymbol{\mathcal{W}}}_i$ from $\check{\boldsymbol{\mathcal{W}}}_i$.

Now returning to the error recursion (190), and computing the expected squared norm, we obtain:

$$\begin{aligned}
\mathbb{E}\,[\|\check{\boldsymbol{\mathcal{W}}}_i\|^2 \,|\, \boldsymbol{\mathcal{F}}_{i-1}] &= \Big\| \mathcal{J}_\epsilon^{\mathsf{T}} \Big(\check{\boldsymbol{\mathcal{W}}}_{i-1} + \mu \check{\boldsymbol{\mathcal{G}}}(\boldsymbol{\mathcal{W}}_{i-1}) \Big) \Big\|^2 + \mu^2 \mathbb{E}\,[\|\mathcal{J}_\epsilon^{\mathsf{T}} \check{\boldsymbol{\mathcal{S}}}_i(\boldsymbol{\mathcal{W}}_{i-1})\|^2 \,|\, \boldsymbol{\mathcal{F}}_{i-1}] \\
&\leq \rho(\mathcal{J}_\epsilon \mathcal{J}_\epsilon^{\mathsf{T}}) \|\check{\boldsymbol{\mathcal{W}}}_{i-1} + \mu \check{\boldsymbol{\mathcal{G}}}(\boldsymbol{\mathcal{W}}_{i-1})\|^2 + \mu^2 \rho(\mathcal{J}_\epsilon \mathcal{J}_\epsilon^{\mathsf{T}}) \mathbb{E}\,[\|\check{\boldsymbol{\mathcal{S}}}_i(\boldsymbol{\mathcal{W}}_{i-1})\|^2 \,|\, \boldsymbol{\mathcal{F}}_{i-1}],
\end{aligned} \tag{194}$$

where, from (Sayed, 2014a, Ch. 9), we know that

$$\rho(\mathcal{J}_\epsilon \mathcal{J}_\epsilon^{\mathsf{T}}) \leq (\rho(J_\epsilon) + \epsilon)^2 < 1. \tag{195}$$

Let us examine the terms in (194). To begin with, note that

$$\begin{aligned}
\rho(\mathcal{J}_\epsilon \mathcal{J}_\epsilon^{\mathsf{T}}) \|\check{\boldsymbol{\mathcal{W}}}_{i-1} + \mu \check{\boldsymbol{\mathcal{G}}}(\boldsymbol{\mathcal{W}}_{i-1})\|^2 &\leq (\rho(J_\epsilon) + \epsilon)^2 \left\| t \frac{1}{t} \check{\boldsymbol{\mathcal{W}}}_{i-1} + \frac{1-t}{1-t} \mu \check{\boldsymbol{\mathcal{G}}}(\boldsymbol{\mathcal{W}}_{i-1}) \right\|^2 \\
&\overset{(a)}{\leq} \frac{(\rho(J_\epsilon) + \epsilon)^2}{t} \|\check{\boldsymbol{\mathcal{W}}}_{i-1}\|^2 + \mu^2 \frac{(\rho(J_\epsilon) + \epsilon)^2}{1-t} \|\check{\boldsymbol{\mathcal{G}}}(\boldsymbol{\mathcal{W}}_{i-1})\|^2 \\
&\overset{(b)}{\leq} (\rho(J_\epsilon) + \epsilon) \|\check{\boldsymbol{\mathcal{W}}}_{i-1}\|^2 + \mu^2 \frac{(\rho(J_\epsilon) + \epsilon)^2}{1 - \rho(J_\epsilon) - \epsilon} \|\check{\boldsymbol{\mathcal{G}}}(\boldsymbol{\mathcal{W}}_{i-1})\|^2,
\end{aligned} \tag{196}$$

where step (a) is because of Jensen's inequality and in step (b) we set $t = \rho(J_\epsilon) + \epsilon < 1$. Next, we bound the square of the sub-gradient term:

$$\begin{aligned}
\|\check{\boldsymbol{\mathcal{G}}}(\boldsymbol{\mathcal{W}}_{i-1})\|^2 &= \|\mathcal{V}_R^{\mathsf{T}} \boldsymbol{\mathcal{G}}(\boldsymbol{\mathcal{W}}_{i-1})\|^2 \\
&\leq \|V_R\|^2 \Big(\sum_{k=1}^N \|g_k(\boldsymbol{w}_{k,i-1})\|^2 \Big) \\
&\leq \|V_R\|^2 \Big(\sum_{k=1}^N e_k^2 \|\widetilde{\boldsymbol{w}}_{k,i-1}\|^2 + f_k^2 \Big) \\
&\overset{(a)}{\leq} \|V_R\|^2 \Big(e_{\max}^2 \|\widetilde{\boldsymbol{\mathcal{W}}}_{i-1}\|^2 + \sum_{k=1}^N f_k^2 \Big),
\end{aligned} \tag{197}$$

where in step (a) we let $e_{\max}^2 = \max_k e_k^2$. We can then bound (196) by

$$\begin{aligned}
\rho(\mathcal{J}_\epsilon \mathcal{J}_\epsilon^{\mathsf{T}}) \|\check{\boldsymbol{\mathcal{W}}}_{i-1} + \mu \check{\boldsymbol{\mathcal{G}}}(\boldsymbol{\mathcal{W}}_{i-1})\|^2 &\leq (\rho(J_\epsilon) + \epsilon) \|\check{\boldsymbol{\mathcal{W}}}_{i-1}\|^2 + \mu^2 \frac{(\rho(J_\epsilon) + \epsilon)^2}{1 - \rho(J_\epsilon) - \epsilon} \|V_R\|^2 \sum_{k=1}^N f_k^2 \\
&\quad + \mu^2 \frac{(\rho(J_\epsilon) + \epsilon)^2}{1 - \rho(J_\epsilon) - \epsilon} \|V_R\|^2 e_{\max}^2 \|\widetilde{\boldsymbol{\mathcal{W}}}_{i-1}\|^2.
\end{aligned} \tag{198}$$

Finally, we consider the last term involving the gradient noise in (194):

$$\begin{aligned}\mathbb{E}\,[\|\check{\boldsymbol{s}}_i(\boldsymbol{\mathcal{W}}_{i-1})\|^2\,|\,\boldsymbol{\mathcal{F}}_{i-1}] &\leq \|V_R\|^2\left(\sum_{k=1}^{N}\beta_k^2\|\widetilde{\boldsymbol{w}}_{k,i-1}\|^2+\sigma_k^2\right)\\ &\leq \|V_R\|^2\beta_{\max}\|\widetilde{\boldsymbol{\mathcal{W}}}_{i-1}\|^2+\|V_R\|^2\sum_{k=1}^{N}\sigma_k^2. \end{aligned}\tag{199}$$

Now introduce the constants:

$$a \triangleq \frac{(\rho(J_\epsilon)+\epsilon)^2}{1-\rho(J_\epsilon)-\epsilon}\|V_R\|^2e_{\max}^2+\rho(J_\epsilon J_\epsilon^{\mathsf{T}})\|V_R\|^2\beta_{\max},\tag{200}$$

$$b \triangleq \frac{(\rho(J_\epsilon)+\epsilon)^2}{1-\rho(J_\epsilon)-\epsilon}\|V_R\|^2\sum_{k=1}^{N}f_k^2+\rho(J_\epsilon J_\epsilon^{\mathsf{T}})\|V_R\|^2\sum_{k=1}^{N}\sigma_k^2.\tag{201}$$

Then, substituting the previous results into (194), we arrive at

$$\mathbb{E}\,\|\check{\boldsymbol{\mathcal{W}}}_i\|^2\leq(\rho(J_\epsilon)+\epsilon)\mathbb{E}\,\|\check{\boldsymbol{\mathcal{W}}}_{i-1}\|^2+\mu^2a\mathbb{E}\,\|\widetilde{\boldsymbol{\mathcal{W}}}_{i-1}\|^2+\mu^2b,\tag{202}$$

In Appendix D we show that $\mathbb{E}\,\|\widetilde{\boldsymbol{\mathcal{W}}}_{i-1}\|^2$, for any iteration i, is bounded by a constant value for sufficient small step-sizes. In this case, we can conclude that

$$\mathbb{E}\,\|\check{\boldsymbol{\mathcal{W}}}_i\|^2\leq(\rho(J_\epsilon)+\epsilon)\mathbb{E}\,\|\check{\boldsymbol{\mathcal{W}}}_{i-1}\|^2+\mu^2b',\tag{203}$$

for some constant b', so that at steady state:

$$\limsup_{i\to\infty}\mathbb{E}\,\|\check{\boldsymbol{\mathcal{W}}}_i\|^2\leq\frac{\mu^2b'}{1-\rho(\mathcal{J}_\epsilon)-\epsilon}=O(\mu^2).\tag{204}$$

Using relation (193), it then follows asymptotically that

$$\mathbb{E}\,\|\widetilde{\boldsymbol{\mathcal{W}}}_i-\bar{\boldsymbol{\mathcal{W}}}_i\|^2 \leq \|V_L\|^2\cdot\mathbb{E}\,\|\check{\boldsymbol{\mathcal{W}}}_i\|^2=O(\mu^2),\tag{205}$$

and, consequently,

$$\mathbb{E}\,\|\widetilde{\boldsymbol{w}}_{k,i}-\bar{\boldsymbol{w}}_i\|^2 \leq \mathbb{E}\,\|\widetilde{\boldsymbol{\mathcal{W}}}_i-\bar{\boldsymbol{\mathcal{W}}}_i\|^2=O(\mu^2).\tag{206}$$

Appendix D. Proof that $\mathbb{E}\,\|\widetilde{\boldsymbol{\mathcal{W}}}_i\|^2$ is uniformly bounded

We follow mathematical induction to establish that $\mathbb{E}\,\|\widetilde{\boldsymbol{\mathcal{W}}}_i\|^2$ is uniformly bounded by a constant value, for all i. Assume, at the initial time instant we have $\mathbb{E}\,\|\widetilde{\boldsymbol{w}}_{k,-1}\|^2<\mathsf{c}$ for all k and for some constant value c. Then, assuming this bound holds at iteration $i-1$, namely,

$$\mathbb{E}\,\|\widetilde{\boldsymbol{w}}_{k,i-1}\|^2\leq\mathsf{c}\quad,\forall k,\tag{207}$$

we would like to show that it also holds at iteration i. Recall from (126) that the diffusion strategy consists of two steps: an adaptation step followed by a combination step. The

adaptation step has a similar structure to the single-agent case. Hence, the same derivation that was used to establish (69) would show that for agent k:

$$2\mu\,(\mathbb{E}\,J_k(\boldsymbol{w}_{k,i-1}) - J_k(w^\star)) \leq\ \alpha_k \mathbb{E}\,\|\widetilde{\boldsymbol{w}}_{k,i-1}\|^2 - \mathbb{E}\,\|\widetilde{\boldsymbol{\psi}}_{k,i}\|^2 + \mu^2(f_k^2+\sigma_k^2), \tag{208}$$

where

$$\alpha_k = 1 - \mu\eta_k + \mu^2(e_k^2+\beta_k^2) = 1 - O(\mu). \tag{209}$$

Now, since $\mathbb{E}\,J_k(\boldsymbol{w}_{k,i-1}) \geq J_k(w^\star)$, we conclude that

$$\begin{aligned}\mathbb{E}\,\|\widetilde{\boldsymbol{\psi}}_{k,i}\|^2 &\leq \alpha_k \mathbb{E}\,\|\widetilde{\boldsymbol{w}}_{k,i-1}\|^2 + \mu^2(f_k^2+\sigma_k^2) \\ &\overset{(207)}{\leq} \alpha_k \mathsf{c} + \mu^2(f_k^2+\sigma_k^2),\end{aligned} \tag{210}$$

where the step-size can be chosen small enough to ensure $\alpha_k \in (0,1)$. Now, it is also clear that there exist sufficiently small values for μ to ensure that, for all agents k:

$$\alpha_k \mathsf{c} + \mu^2(f_k^2+\sigma_k^2) \leq \mathsf{c}, \tag{211}$$

which then guarantees that

$$\mathbb{E}\,\|\widetilde{\boldsymbol{\psi}}_{k,i}\|^2 \leq \mathsf{c}. \tag{212}$$

It then follows from the combination step (126) that

$$\begin{aligned}\mathbb{E}\,\|\widetilde{\boldsymbol{w}}_{k,i}\|^2 &= \mathbb{E}\,\left\|\sum_{\ell\in\mathcal{N}_k} a_{\ell k}\widetilde{\boldsymbol{\psi}}_{\ell,i}\right\|^2 \\ &\leq \sum_{\ell\in\mathcal{N}_k} a_{\ell k}\mathbb{E}\,\left\|\widetilde{\boldsymbol{\psi}}_{\ell,i}\right\|^2 \\ &\leq \sum_{\ell\in\mathcal{N}_k} a_{k\ell}\mathsf{c} \\ &= \mathsf{c},\ \ \forall k.\end{aligned} \tag{213}$$

Therefore, starting from (207), we conclude that $\mathbb{E}\,\|\widetilde{\boldsymbol{w}}_{k,i}\|^2 < \mathsf{c}$ as well, as desired. Finally, since $\mathbb{E}\,\|\widetilde{\boldsymbol{\mathcal{W}}}_i\|^2 = \sum_{k=1}^N \mathbb{E}\,\|\widetilde{\boldsymbol{w}}_{k,i}\|^2$, we conclude that $\mathbb{E}\,\|\widetilde{\boldsymbol{\mathcal{W}}}_i\|^2$ is also uniformly bounded over time.

References

A. Agarwal, P. L. Bartlett, P. Ravikumar, and M. J. Wainwright. Information-theoretic lower bounds on the oracle complexity of stochastic convex optimization. *IEEE Trans. Inf. Theory*, 58(5):3235–3249, May 2012.

F. Bach, R. Jenatton, J. Mairal, and G. Obozinski. Optimization with sparsity-inducing penalties. *Foundations and Trends in Machine Learning*, 4(1):1–106, 2012.

A. Beck and M. Teboulle. Fast gradient-based algorithms for constrained total variation image denoising and deblurring problems. *IEEE Trans. Image Process.*, 18(11):2419–2434, 2009a.

A. Beck and M. Teboulle. A fast iterative shrinkage-thresholding algorithm for linear inverse problems. *SIAM J. Imag. Sci.*, 2(1):183–202, 2009b.

D. P. Bertsekas. *Nonlinear Programming*. Athena scientific Belmont, 1999.

C. M. Bishop. *Pattern Recognition and Machine Learning*. Springer, 2006.

L. Bottou. Large-scale machine learning with stochastic gradient descent. In *Proc. of COMPSTAT*, pages 177–186. Springer, 2010.

L. Bottou. Stochastic gradient tricks. In G. Montavon, G. B. Orr, and K. Müller, editors, *Neural Networks, Tricks of the Trade, Reloaded*, Lecture Notes in Computer Science (LNCS 7700), pages 430–445. Springer, 2012.

O. Bousquet and L. Bottou. The tradeoffs of large scale learning. In *Advances in Neural Information Processing Systems(NIPS), 20*, pages 161–168. 2008.

S. Boyd and A. Mutapcic. Stochastic subgradient methods. *Lecture Notes for EE364b, Stanford University,*, 2008.

F. S. Cattivelli and A. H. Sayed. Diffusion LMS strategies for distributed estimation. *IEEE Trans. Signal Process.*, 58(3):1035–1048, 2010.

C.-C. Chang and C.-J. Lin. LIBSVM: A library for support vector machines. *ACM Trans. on Intelligent Systems and Tech.*, 2:27:1–27:27, 2011.

J. Chen and A. H. Sayed. On the learning behavior of adaptive networks—Part I: Transient analysis. *IEEE Trans. Inf. Thy.*, 61(6):3487–3517, June 2015a.

J. Chen and A. H. Sayed. On the learning behavior of adaptive networks—Part II: Performance analysis. *IEEE Trans. Inf. Thy.*, 61(6):3518–3548, June 2015b.

S. S. Chen, D. L. Donoho, and M. A. Saunders. Atomic decomposition by basis pursuit. *SIAM journal on scientific computing*, 20(1):33–61, 1998.

Y. Chen, Y. Gu, and A. O. Hero. Sparse LMS for system identification. In *Proc. IEEE ICASSP*, pages 3125–3128, Taipei, Taiwan, 2009.

S. Chouvardas, K. Slavakis, Y. Kopsinis, and S. Theodoridis. A sparsity promoting adaptive algorithm for distributed learning. *IEEE Trans. Signal Process.*, 60(10):5412–5425, Oct. 2012.

C. Cortes and V. Vapnik. Support-vector networks. *Machine learning*, 20(3):273–297, 1995.

P. Di Lorenzo and A. H. Sayed. Sparse distributed learning based on diffusion adaptation. *IEEE Trans. Signal Process.*, 61(6):1419–1433, March 2013.

P. Di Lorenzo, S. Barbarossa, and A. H. Sayed. Sparse diffusion LMS for distributed adaptive estimation. In *Proc. IEEE Int. Conf. Acoust. Speech Signal Process. (ICASSP)*, pages 3281–3284, Kyoto, Japan, Mar. 2012.

D. L. Donoho and J. M. Johnstone. Ideal spatial adaptation by wavelet shrinkage. *Biometrika*, 81(3):425–455, 1994.

D. L. Donoho, M. Elad, and V. N. Temlyakov. Stable recovery of sparse overcomplete representations in the presence of noise. *IEEE Trans. Inf. Theory*, 52(1):6–18, 2006.

D. L. Duttweiler. Proportionate normalized least-mean-squares adaptation in echo cancelers. *IEEE Trans. Speech and Audio Process.*, 8(5):508–518, Sep. 2000.

T. Hastie, R. Tibshirani, and J. Friedman. *The Elements of Statistical Learning*. Springer, 2009.

S. Kar and J. M. F. Moura. Distributed consensus algorithms in sensor networks with imperfect communication: Link failures and channel noise. *IEEE Trans. Signal Process.*, 57(1):355–369, 2009.

J. E. Kelley. The cutting-plane method for solving convex programs. *Journal of the Society for Industrial and Applied Mathematics*, pages 703–712, 1960.

K. Kiwiel. *Methods of Descent for Non-differentiable Optimization*. Springer-Verlag, 1985.

Y. Kopsinis, K. Slavakis, and S. Theodoridis. Online sparse system identification and signal reconstruction using projections onto weighted balls. *IEEE Trans. Signal Process.*, 59(3): 936–952, Mar. 2011.

A. J. Laub. *Matrix Analysis for Scientists and Engineers*. SIAM, 2005.

Y. Liu, C. Li, and Z. Zhang. Diffusion sparse least-mean squares over networks. *IEEE Trans. Signal Process.*, 60(8):4480–4485, Aug. 2012.

C. D. Meyer. *Matrix Analysis and Applied Linear Algebra*. SIAM, 2000.

E. Moulines and F. Bach. Non-asymptotic analysis of stochastic approximation algorithms for machine learning. In *Advances in Neural Information Processing Systems(NIPS), 24*, pages 451–459. Curran Associates, Inc., 2011.

Y. Murakami, M. Yamagishi, M. Yukawa, and I. Yamada. A sparse adaptive filtering using time-varying soft-thresholding techniques. In *Proc. IEEE Int. Conf. Acoust. Speech Signal Process. (ICASSP)*, pages 3734–3737, Dallas, TX, 2010.

A. Nedic. Subgradient methods for convex minimization, May 2002.

A. Nedic and A. Ozdaglar. Distributed subgradient methods for multi-agent optimization. *IEEE Trans. Autom. Control*, 54(1):48–61, 2009.

A. Nemirovski, A. Juditsky, G. Lan, and A. Shapiro. Robust stochastic approximation approach to stochastic programming. *SIAM J. Optm.*, 19(4):1574–1609, 2009.

Y. Nesterov. *Introductory Lectures on Convex Optimization*. Springer, 2004.

N. Parikh and S. Boyd. Proximal algorithms. *Foundations and Trends in optimization*, 1 (3):123–231, 2013.

J. Platt. Fast training of support vector machines using sequential minimal optimization. *Advances in Kernel Methods—Support Vector Learning*, 3, 1999.

B. T. Polyak. *Introduction to Optimization*. Optimization Software New York, 1987.

S. S. Ram, A. Nedić, and V. V. Veeravalli. Distributed stochastic subgradient projection algorithms for convex optimization. *J. Optm. Theory and Appl.*, 147(3):516–545, 2010.

L. I. Rudin, S. Osher, and E. Fatemi. Nonlinear total variation based noise removal algorithms. *Physica D: Nonlinear Phenomena*, 60(1):259–268, 1992.

A. H. Sayed. *Adaptive Filters*. John Wiley & Sons, 2008.

A. H. Sayed. Adaptation, learning, and optimization over networks. *Foundations and Trends in Machine Learning*, 7(4-5):311–801, 2014a.

A. H. Sayed. Adaptive networks. *Proceedings of the IEEE*, 102(4):460–497, 2014b.

S. Shalev-Shwartz, Y. Singer, N. Srebro, and A. Cotter. Pegasos: Primal estimated subgradient solver for SVM. *Mathematical Programming*, 127(1):3–30, 2011.

N. Z. Shor. *Minimization Methods for Non-differentiable Functions*, volume 3. Springer-Verlag, 2012.

S. Theodoridis and K. Koutroumbas. *Pattern Recognition*. Academic Press, 4th edition, 2008.

R. Tibshirani. Regression shrinkage and selection via the lasso. *Journal of the Royal Statistical Society, Series B (Methodological)*, pages 267–288, 1996.

Z. J. Towfic and A. H. Sayed. Stability and performance limits of adaptive primal-dual networks. *IEEE Trans. Signal Process.*, 63(11):2888–2903, June 2015.

S.-Y. Tu and A. H. Sayed. Diffusion strategies outperform consensus strategies for distributed estimation over adaptive networks. *IEEE Trans. Signal Process.*, 60(12):6217–6234, 2012.

V. Vapnik. *Statistical Learning Theory*. Wiley NY, 1998.

R. Wets. Stochastic programming. In G. Nemhauser and A. Rinnnooy Kan, editors, *Handbook for Operations Research and Mangement Sciences*, volume 1, pages 573–629. Elsevier, 1989.

W. Yu, G. Chen, Z. Wang, and W. Yang. Distributed consensus filtering in sensor networks. *IEEE Trans. on Systems, Man, and Cybernetics, Part B: Cybernetics*, 39(6):1568–1577, 2009.